Department of Electronic & Telecommunication Engineering
University of Moratuwa

BM4151 – Biosignal Processing

Name: Sahan Sulochana Hettiarachchi
Index: **180237G**

This is submitted as a partial fulfilment for the module BM4151 – Biosignal Processing

25th of November 2022

1 Smoothing Filters

Smoothing filters are applied to pass required low frequencies and attenuate high pass frequency components (high-frequency noises). In this report, Two types of smoothing filters will be discussed.

1.1 Moving Average filters

The following equation shows the derived output signal of the x(n) signal after applying the Moving average signal.

$$y(n) = \frac{1}{N}\sum_{k=0}^{N-1} x(n-k)$$

In this filter implementation, we will be adding a moving average filter to the noise-added signal ECG signal of sampling frequency 500Hz.

First, we will load the ECG data file "ECG_template.mat" to the workspace. The characteristic waveform of the ECG waveform is as follows(Figure 1).

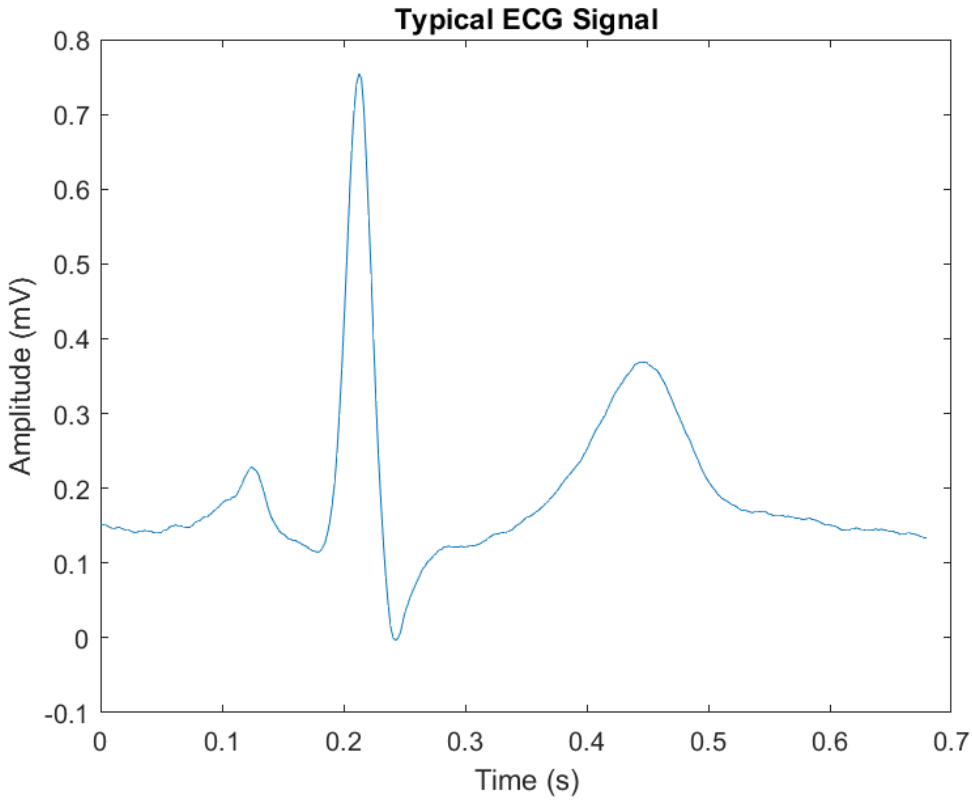

Figure 1: Typical ECG signal

Typical characteristics of an ECG waveform (. P wave, QRS complex and T wave) can be identified the in the above figure. Then 5dB additive gaussian noise is added to the raw ECG signal and it is defined as the 'nECG'. Figure 2 shows the noise-added signal(nECG) and the original signal(ECG).

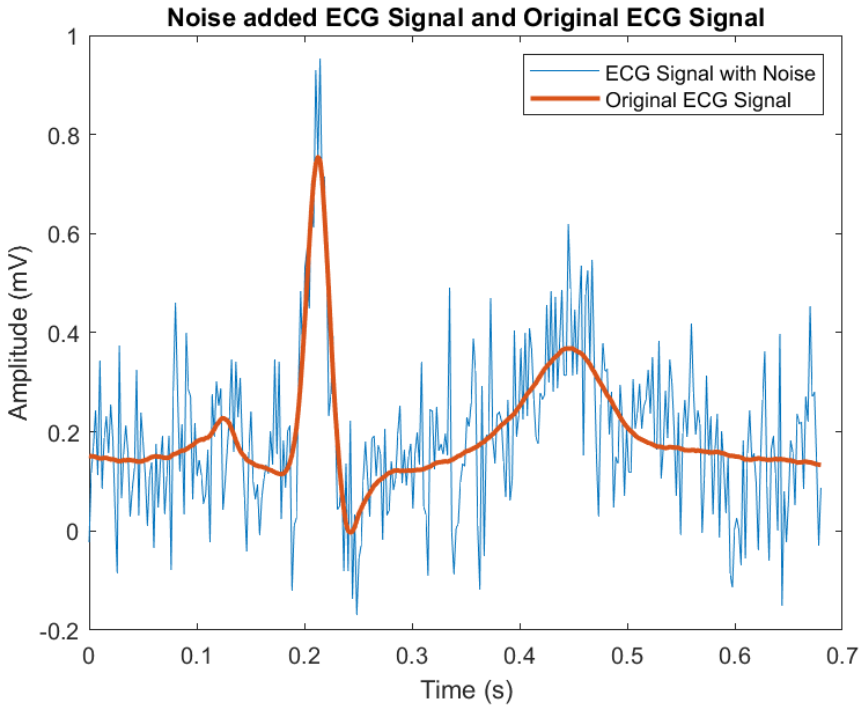

Figure 2:Noise added ECG Signal and Original ECG Signal

Next, consider the Power Spectral Density of the noise-added ECG signal and the original ECG signal.

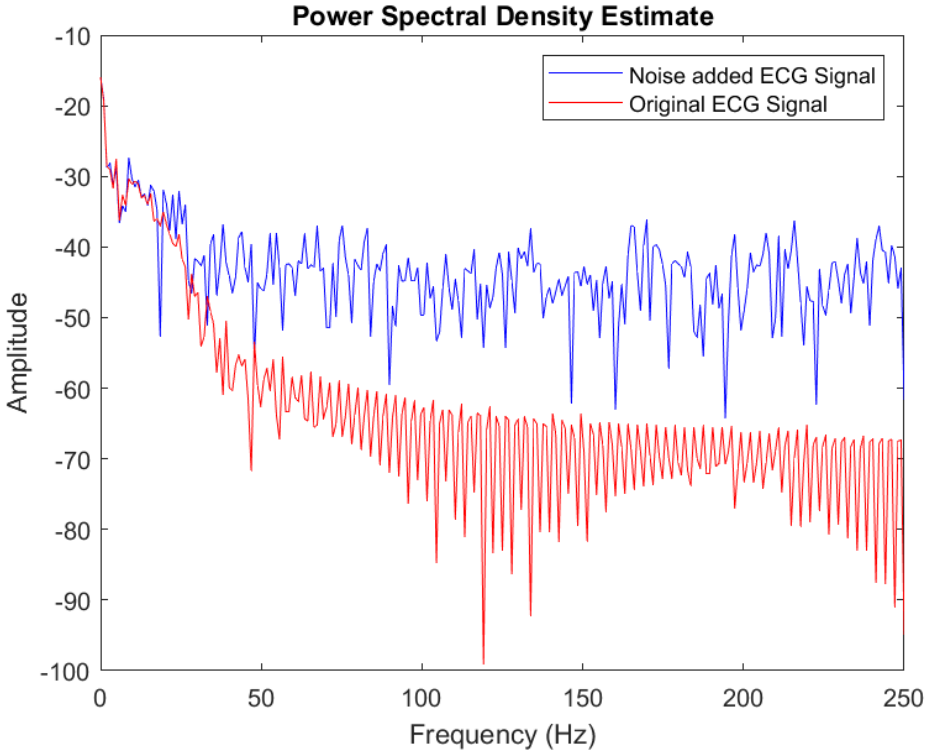

Figure 3:Power Spectral Density of Original ECG and noise added ECG

According to Figure 3, the low-frequency component of the original signal has higher amplitudes (high power) compared to the higher-frequency components of the original signal. Noise-added signal has more power compared to the original ECG signal.

1.1.1 MA(3) filter implementation with a customised script

Deriving the group delay

$$Group\ Delay(\tau_g) = \frac{-\partial Arg\big(H(\omega)\big)}{\partial \omega}$$

Let's consider the transfer function of the moving average filter (Filter order is **N**),

$$H(\omega) = \frac{1}{N}\sum_{k=0}^{N-1} e^{-jk\omega}$$

$$H(\omega) = \frac{e^{-j\left(\frac{N-1}{2}\right)\omega}}{N}\sum_{k=-(N-1)/2}^{(N-1)/2} e^{-jk\omega}$$

By substituting for $e^{jk\omega} = \cos(k\omega) + jsin(k\omega)$,

$$H(\omega) = \left(\frac{\cos\left(\frac{(N-1)\omega}{2}\right) - jsin\left(\frac{(N-1)\omega}{2}\right)}{N}\right)\sum_{k=-(N-1)/2}^{(N-1)/2} 2\cos(k\omega)\, Arg\big(H(\omega)\big)$$

$$= \tan^{-1}\left(\frac{Im\big(H(\omega)\big)}{Re\big(H(\omega)\big)}\right) = \tan^{-1}\left(\frac{\cos\left(\frac{N-1}{2}\right)\omega}{-\sin\left(\frac{N-1}{2}\right)\omega}\right)$$

$$Arg\big(H(\omega)\big) = \frac{-N\omega}{2}$$

$$Group\ Delay\ (\tau_g) = \frac{-\partial Arg\big(H(\omega)\big)}{\partial \omega} = \frac{\boldsymbol{N-1}}{\boldsymbol{2}}$$

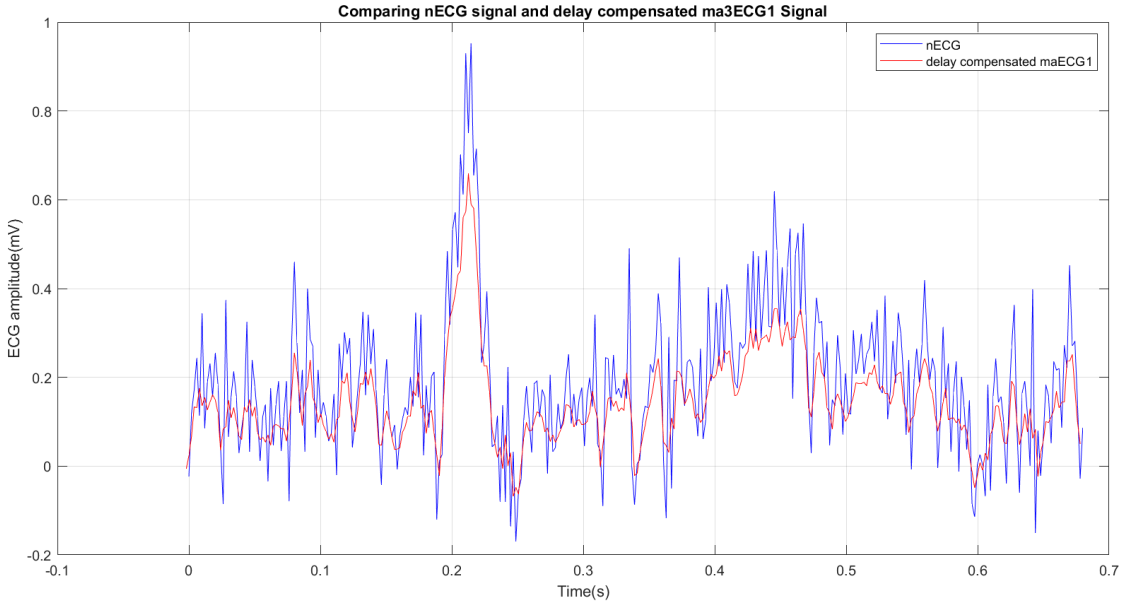

Figure 4:Noise added ECG signal and delay compensated MA(3) output signal

The filtered signal amplitude has been reduced compared to the original signal and also high-frequency variation has been reduced. The filtered signal has been smoothened. The group delay of the current filter is one.

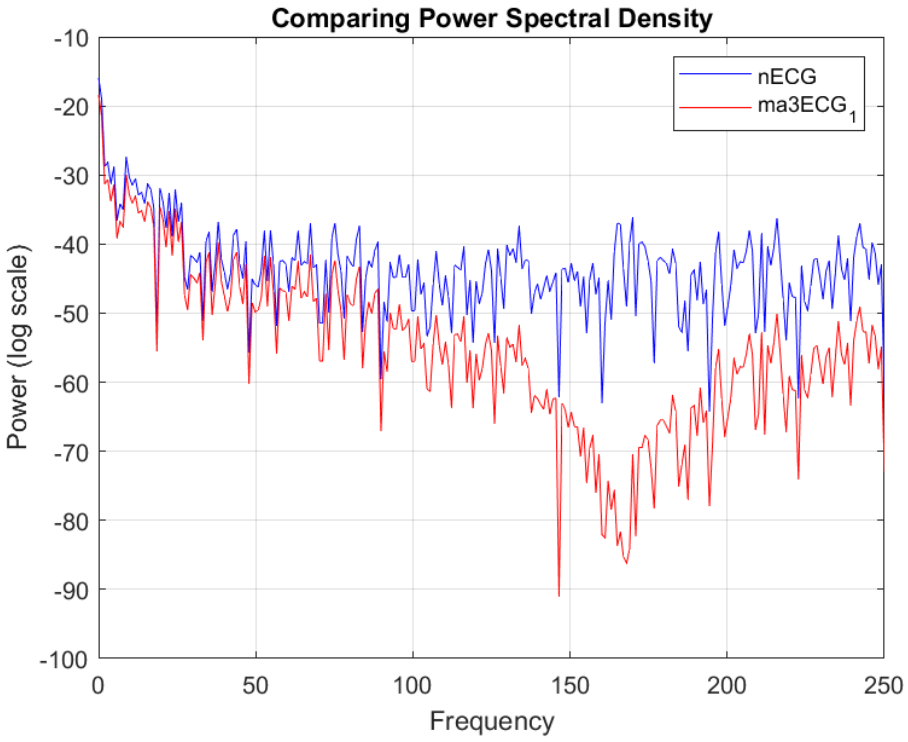

Figure 5:Power Spectral Density of the nECG and ma3ECG_1

Power Spectral Density figures show that the power of the high-frequency component of the filtered signal has been reduced compared to the noise-added ECG signal. Therefore using MA(3) filters noise can be reduced and obtained require signals.

1.1.2 MA(3) filter implementation with the MATLAB built-in function

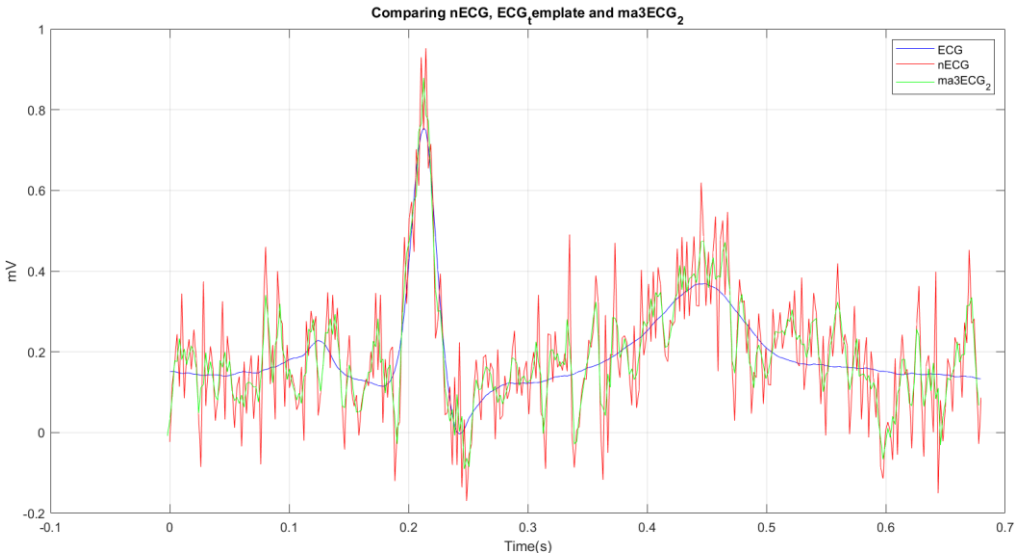

Figure 6: Comparing nECG, ECG_template and ma3ECG_2

Figure 6 shows the original ECG signal, noise-added signal and filtered ECG signal. Filtered signal amplitude has reduced compared to the noise-added ECG signal but is still higher than to original ECG signal.

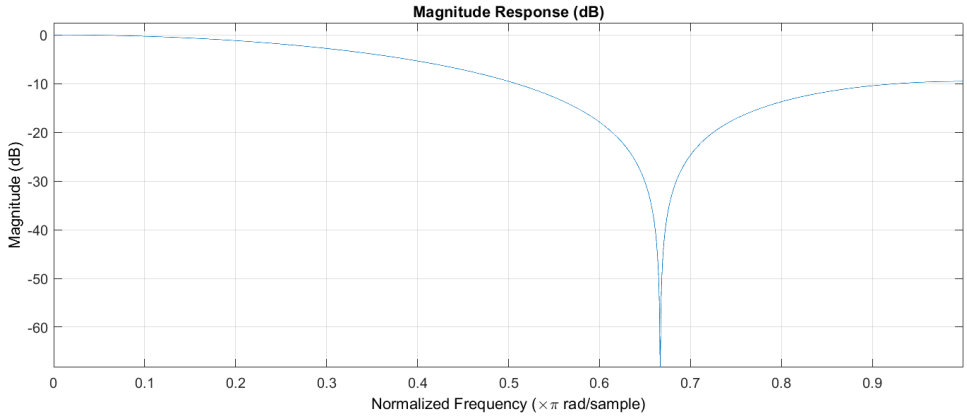

Figure 8: Magnitude Response

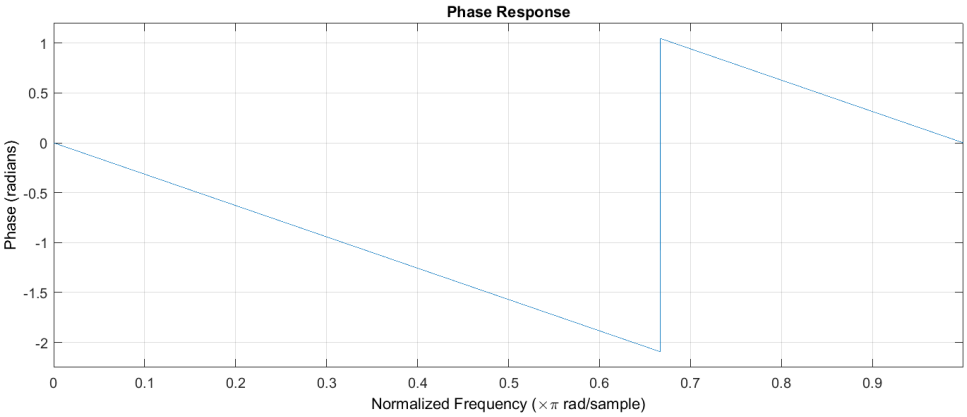

Figure 9:Phase response

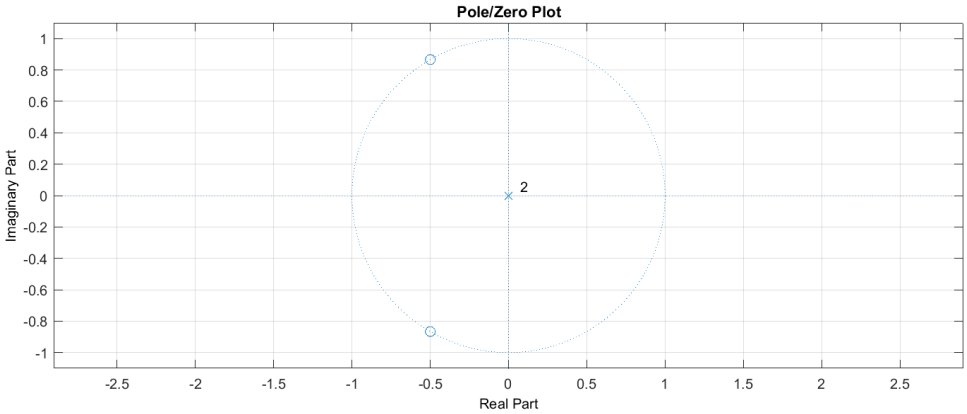

Figure 7: Pole Zero Plot

1.1.3 MA(10) filter implementation with the MATLAB built-in function

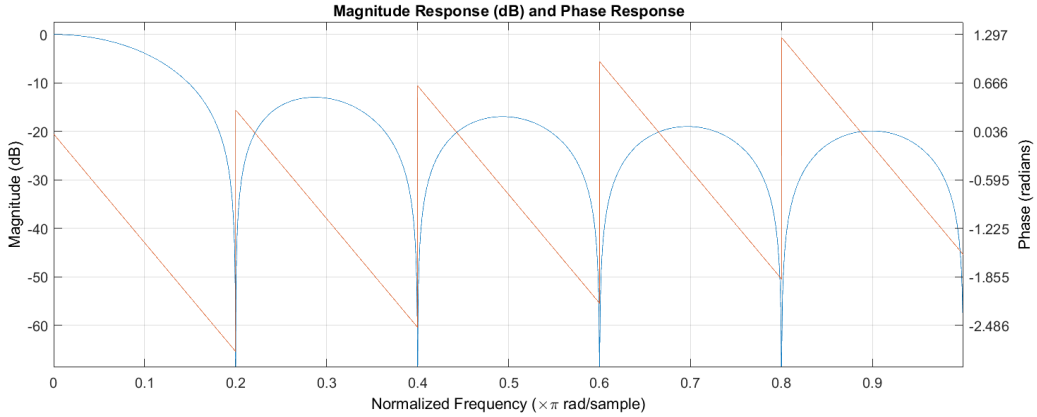

Figure 10:Magnitude and phase response of MA(10) filter

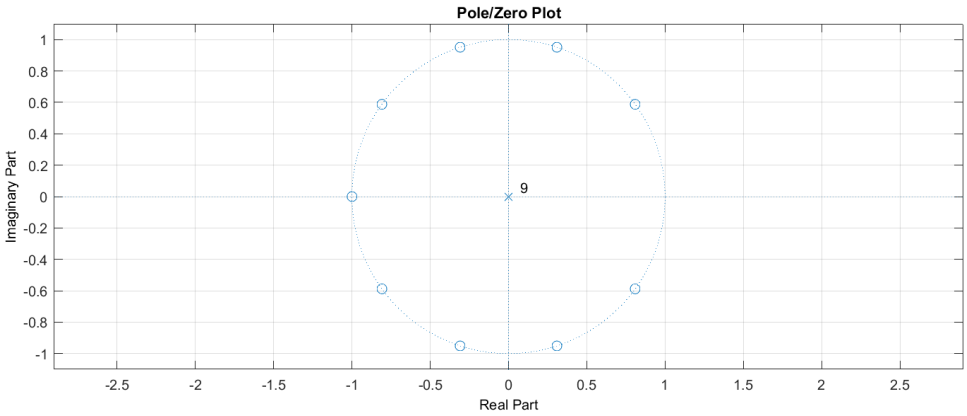

Figure 12: Pole Zero plot of the MA(10) filter

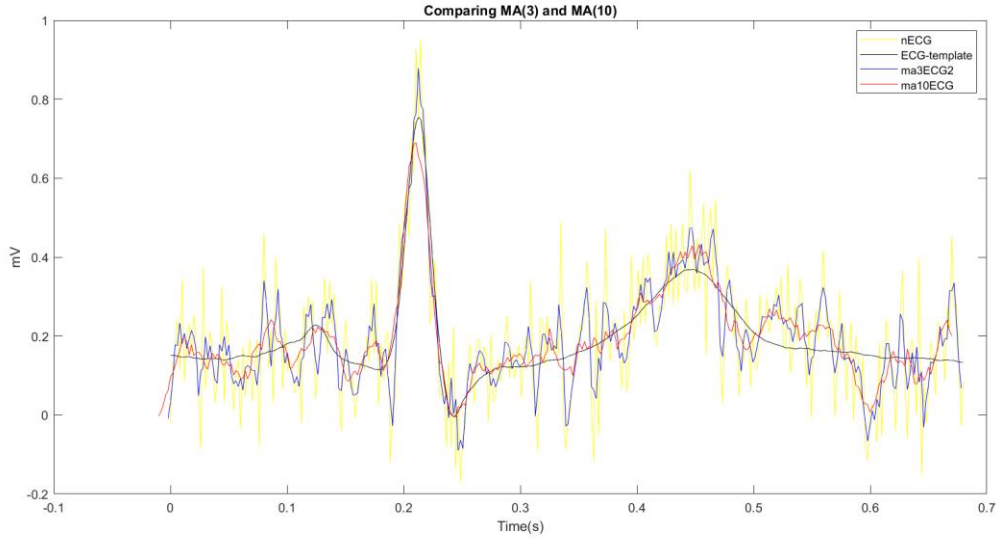

Figure 11: Original ECG, Noise ECG, ma3ECG_2 and ma10ECG

Figure 11 has shown the MA(10) filter is smoother, and more filtered compared to MA(3) filter and more high-frequency noises are attenuated compared to MA(3). Furtherly -3dB attenuation of the

MA(3) is about 0.3 of the normalized frequency and when it comes to the MA(10) it is about 0.08 of the normalized frequency.

Most useful details of the ECG signals are contained in lower frequency components. Higher frequency components contained more noise. The increment of the filter order has led to reducing more high-frequency noises. Therefore amplitude levels of the MA(10) have reduced compared to the MA(3). MA(10) has been able to reduce noise compared to MA(3).

1.1.4 Optimum MA(N) filter order

Although increasing the filter order reduces noises, it also causes to smooths the peaks of the original, not noise signals. Therefore it may miss useful information about the signal. In that case, the importance of the optimum filter order occurred. The following Figure 13 shows the mean squared error concerning filter order.

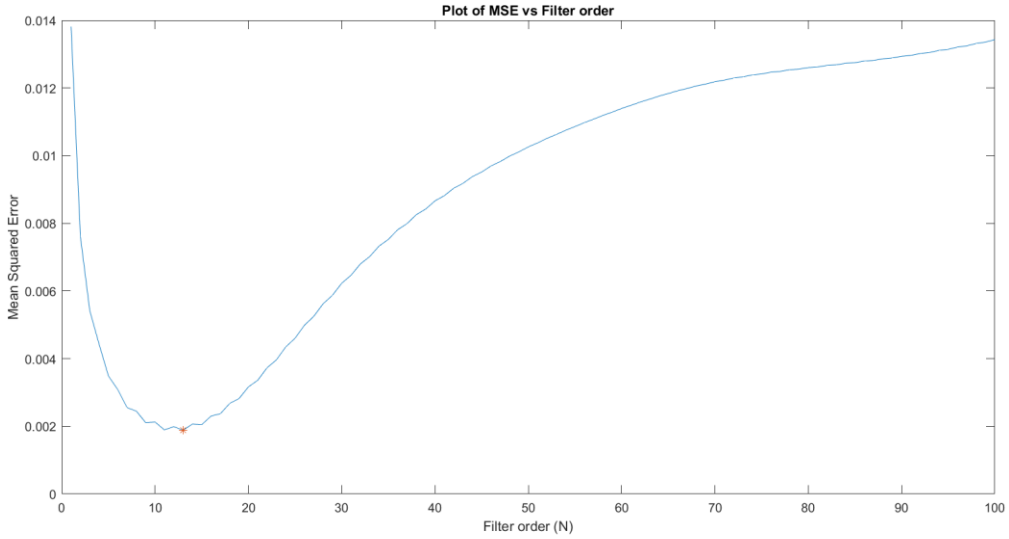

Figure 13: MA filter order vs MSE

According to Figure 13, the optimum filter order is at **11.** Initially, the MSE is decreasing with the increment of the filter order and after passing the optimum filter order it increases the MSE with the filter order.

When increasing the filter order of the MA filters removes high-frequency components of the signal. As mentioned previously if the limit is exceeded the required frequency components are also removed. Then MSE is increasing when the expected signal is not received. Therefore it is important to have an optimum filter order when using MA filters.

1.2 Savitzky-Golay SG(N,L) filter

1.2.1 Application of SG(N,L)

Savitzky-Golay filters are a type of smoothing filter that works by fitting a polynomial function to a set of data points. The order of the polynomial function is the order of the filter (N), and the filter length (L) sets the number of data points to be 2L +1.

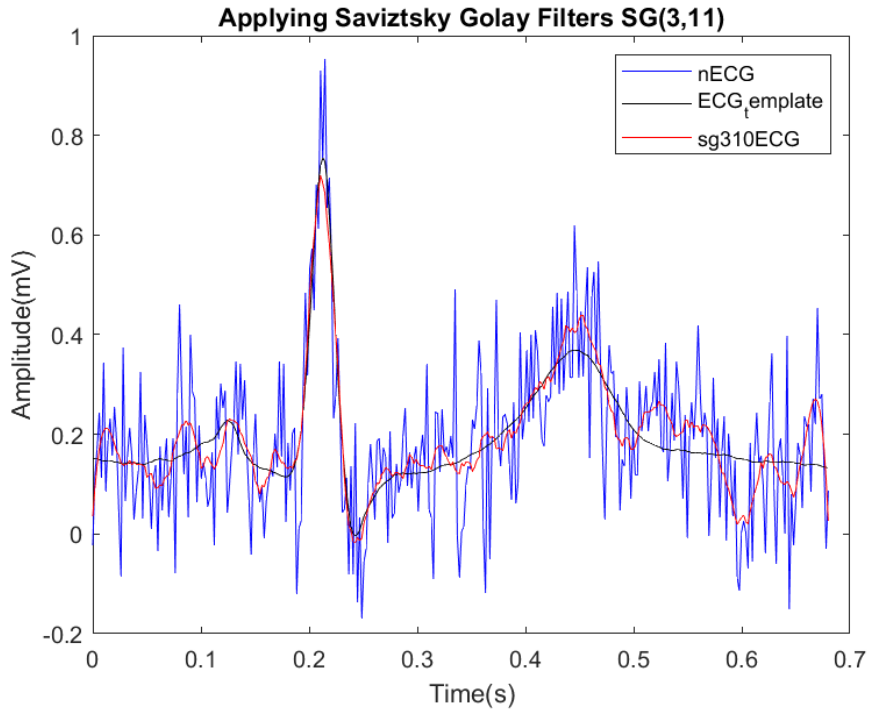

Figure 14: nECG, ECG and sg310ECG signal

By observing Figure 14, we can verify that the Savitzky-Golay filter SG(3,11) has reduced the noise and it behaves as a smoothing filter.

Figure 15: Optimum Filter Order vs MSE vs Length of Savitzky-Golay filter

The **optimum filter order** is **4** and the **optimum length** of the window is **17**.

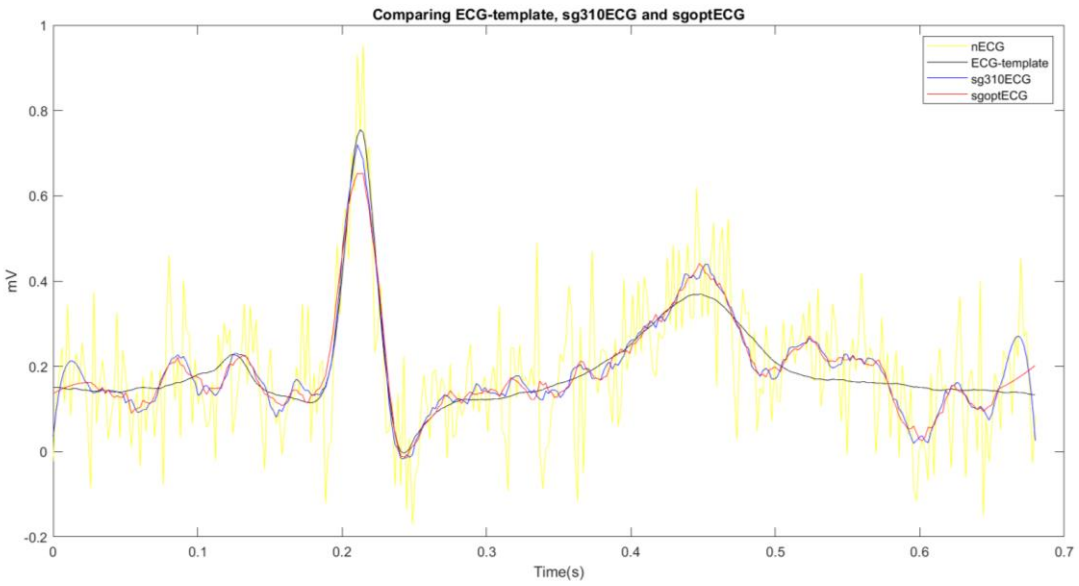

Figure 16:Comparing ECG-template, sg310ECG and sgoptECG

Figure 16 has shown the Savitzky-Golay filter generated a more smooth and filtered signal compared to the MA filters. When it comes to the computation complexity of the two filters, the filter coefficients of the Savitzky-Golay filter are required to calculate but in MA filters filter coefficients are constant. Therefore MA filters are required less time compare to Savitzky-Golay filters.

2 Ensemble Averaging

2.1 Signal with multiple measurements

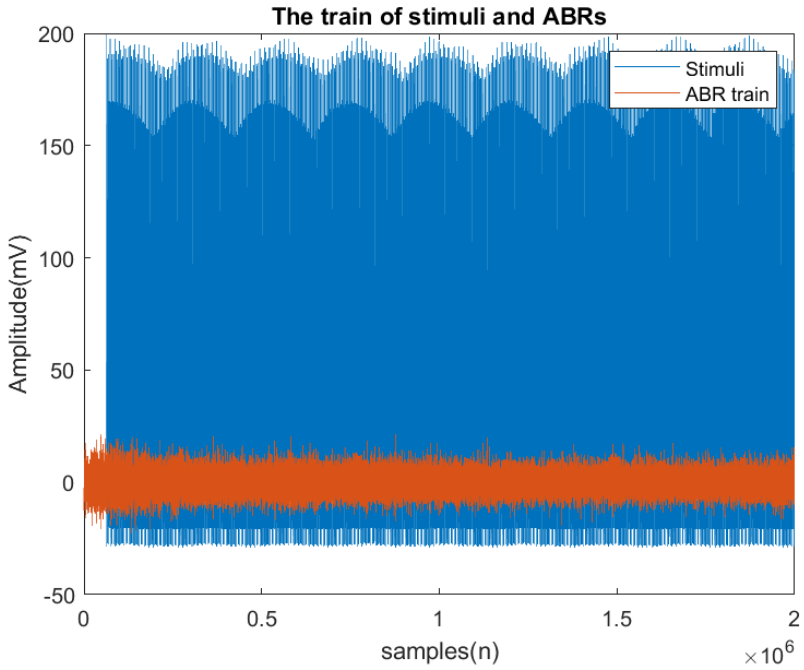

Figure 17:Train of ABR recording and Audio pulse stimuli

Figure 17 shows the train of the ABR recording and audio pulse stimuli. Figure 18 shows the zoomed view of the graphs.

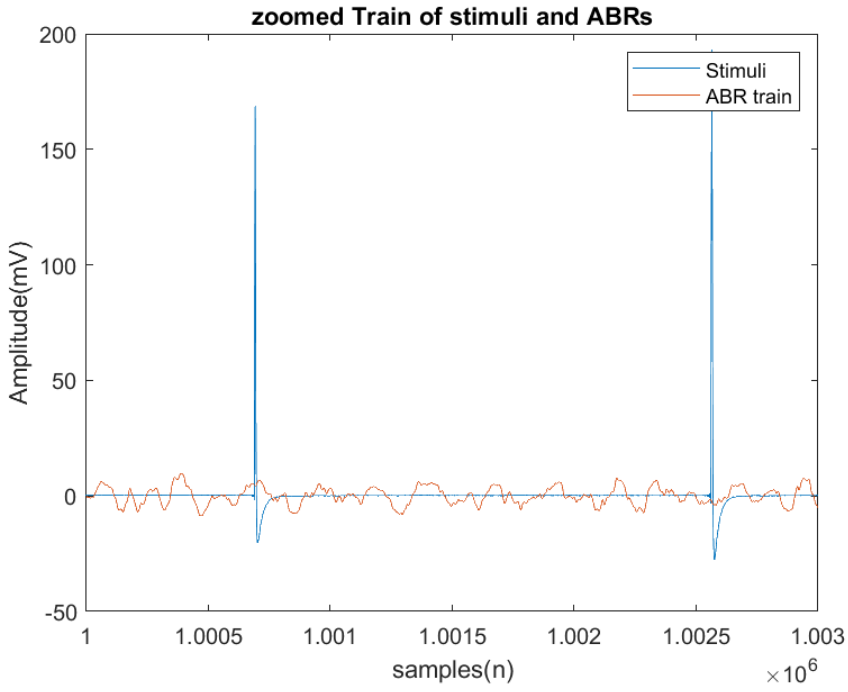

Figure 18:Zoomed Train of stimuli and ABRs

Because the stimuli trigger ABR, we may use the stimulus beginning points to split the ABR train into repeated patterns. To extract ABR epochs, we will use a time window of 12ms (-2ms to +10ms from the stimulus time point). The retrieved epochs' ensemble average is displayed below.

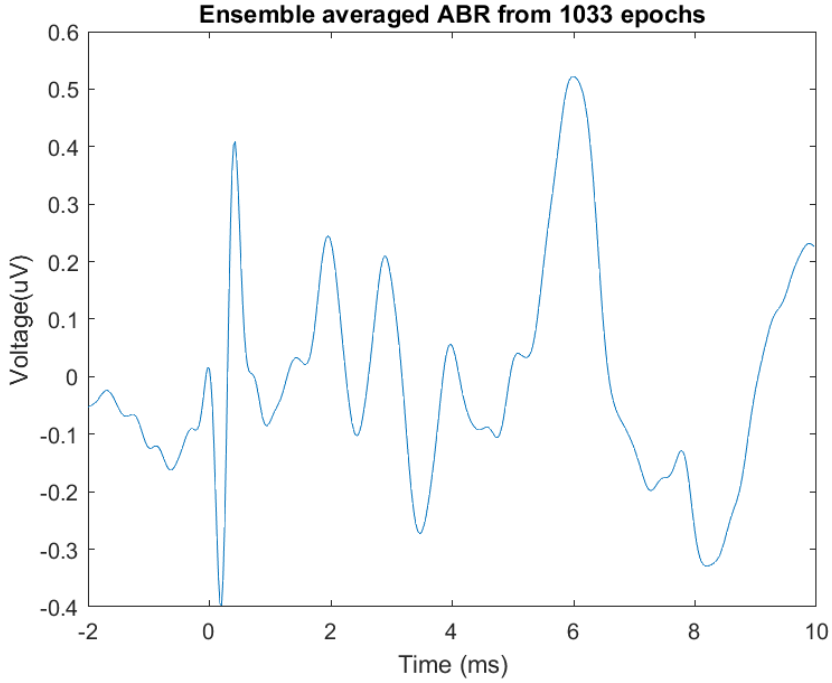

Figure 19:Ensemble averaged ABR from1033 epochs

2.1.1 Improvement of SNR

In the implementation, we have calculated the MSE with the given number of epochs. Figure 20 shows the MSE value concerning the number of epochs.

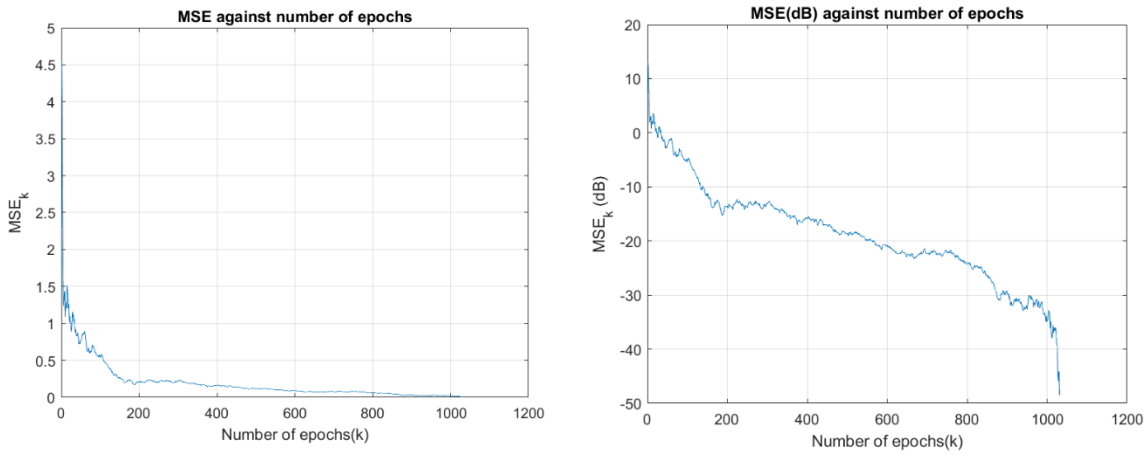

Figure 20: MSE vs number of epochs

The figures verify that when the number of epochs is increasing the MSE is converging to zero. Even when k=1000 the MSE value is almost 0. In the logarithmic plot also this can be visualized. Therefore in a high number of epochs, the practical values reach theoretical values.

Theoretical values can be obtained as follows,

Let's consider the standard deviation of the signal epoch is S_i and in each epoch, the standard deviation of the signal will be the same. Therefore the total summation of the standard deviation is $S_k = kS_i$ for k number of epochs.

$$S_1 = \sum_{j=1}^{k} S_i = kS_i$$

In each epoch, the same signal is received. Therefore variance is dependent only on the noise. In a single epoch, the standard deviation of the noise is σ_i. The standard deviation of the noise(σ_k) can be calculated as follows.

$$\sigma_k{}^2 = \sum_{j=1}^{k} \sigma_i^2 = k\sigma_i^2$$

$$\sigma_k = \sqrt{k}\sigma_i$$

SNR of the signal can be calculated as follows,

$$SNR_k = \frac{S_k}{\sigma_k} = \frac{kS_i}{\sqrt{k}\sigma_k} = \sqrt{k}\frac{S_i}{\sigma_i} = \sqrt{k}\, SNR_j$$

From this derived equation, we can verify that number of the epoch and SNR has proportional relation to each other. The logarithmic scale value of the SNR can be calculated as follows.

$$SNR_k = \frac{1}{2}\,(20\log k) + 20\log\left(SNR_j\right)$$

$$SNR_k = 10\log(k) + 20\log(SNR_j)$$

Figure 21 shows the SNR variation concerning a number of epochs.

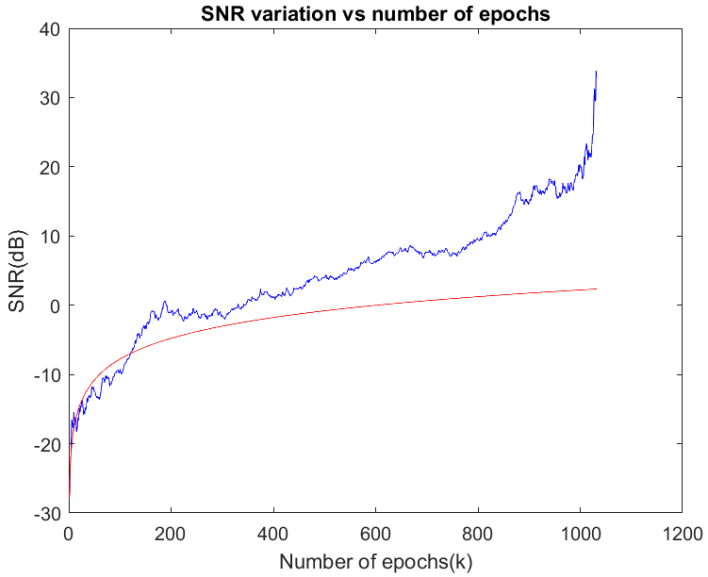

Figure 21: SNR variation vs number of epochs

2.2 Signal with repetitive patterns

2.2.1 Viewing the signal and addition Gaussian white noise

Figure 22 shows the ECG waveform of a dataset. For clear observation, the figure is zoomed in (Figure 23)

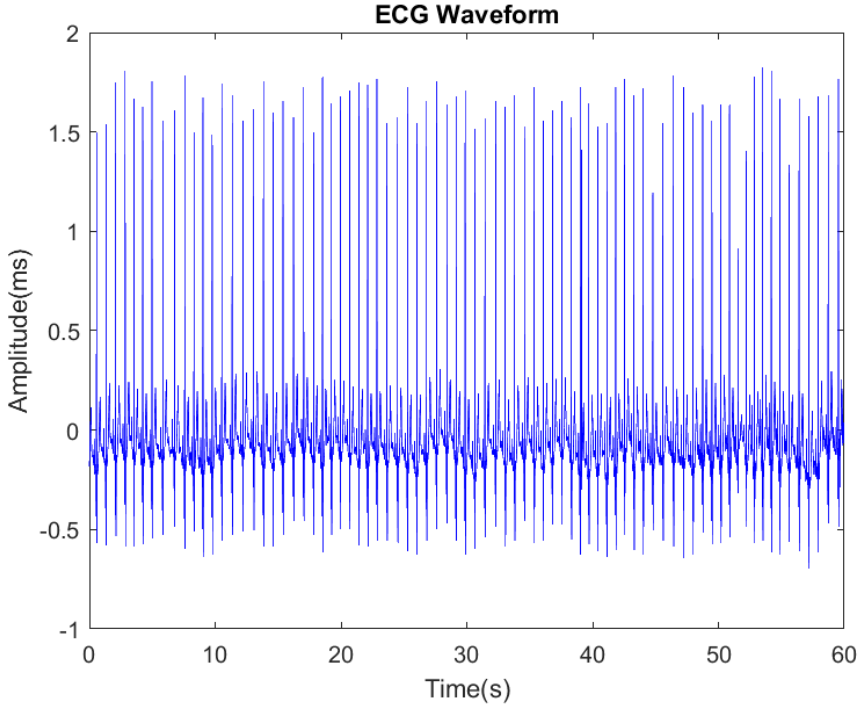

Figure 22:ECG Waveform

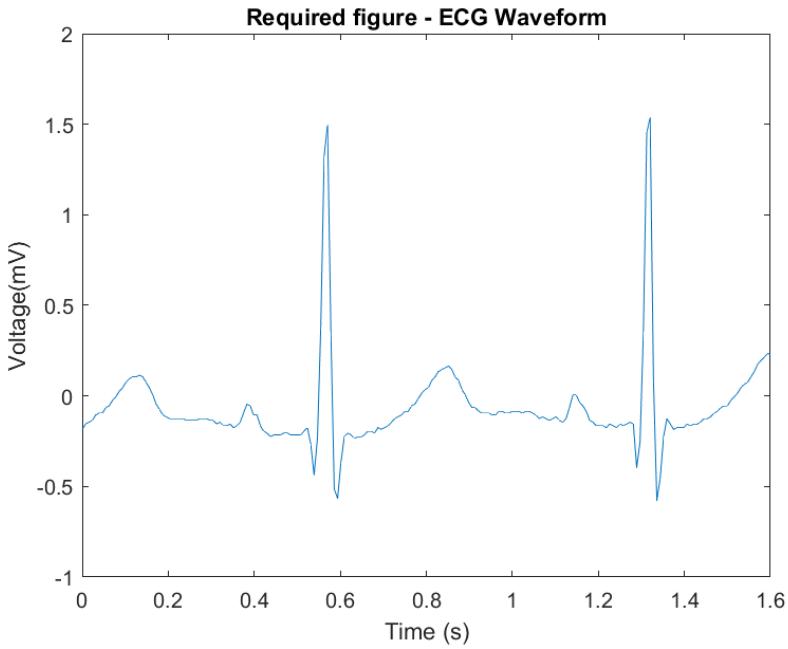

Figure 23: Zoomed figure of the ECG signal

Consecutive signal peaks contain 100 data points. Therefore one sample of 100 consecutive data points is selected as the 'ECG_template'. In this implementation 40 to 139 data points are selected as the data sample. Figure 24 shows the waveform for selected data points.

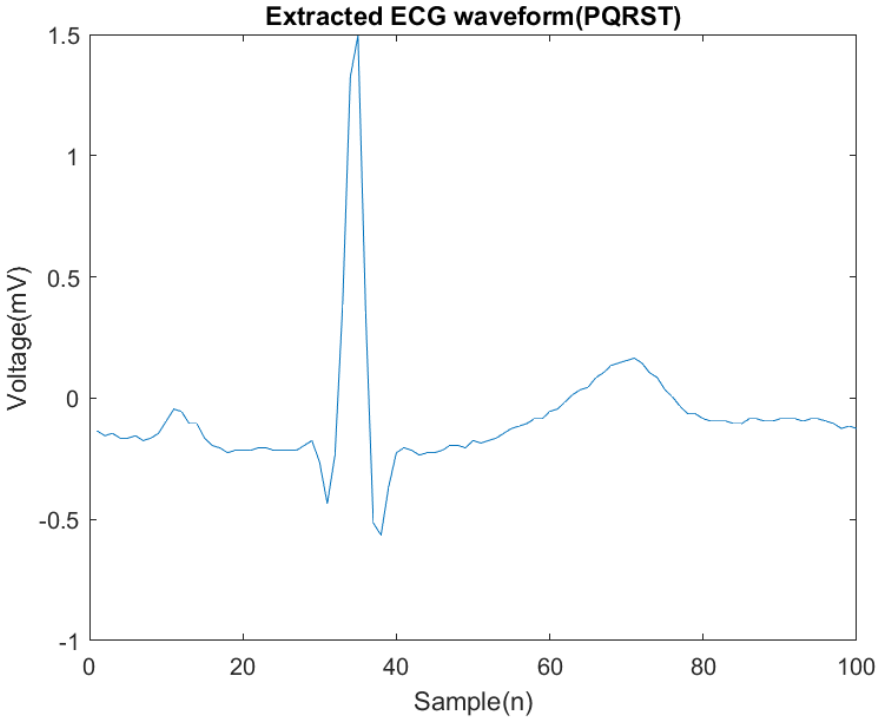

Figure 24: Extracted ECG waveform (40-139)

In the above ECG signal, the PQRST waveform can be identified. Then 5dB additive gaussian noise will be added to the 'ECG_tempalate' signal. Figure 25 shows the noise-added ECG signal.

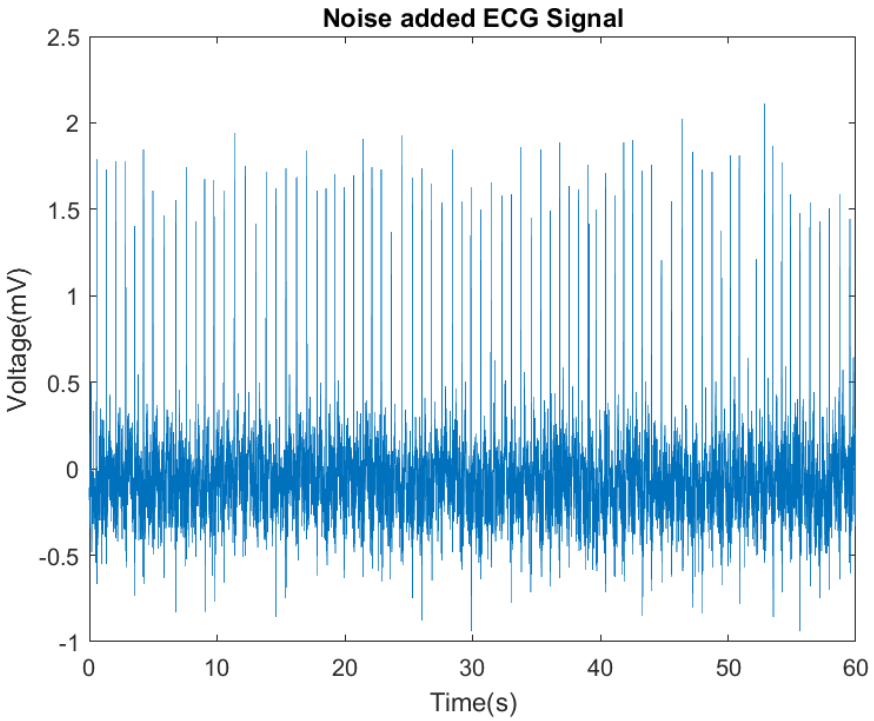

Figure 25: Noise added ECG signal

2.2.2 Segmenting ECG into separate epochs and ensemble averaging

Given that an ECG template already exists, it is preferable to use points of the highest correlation with a noisy ECG pulse train to segment the ECG pulse train into discrete epochs rather than just recognizing the R wave.

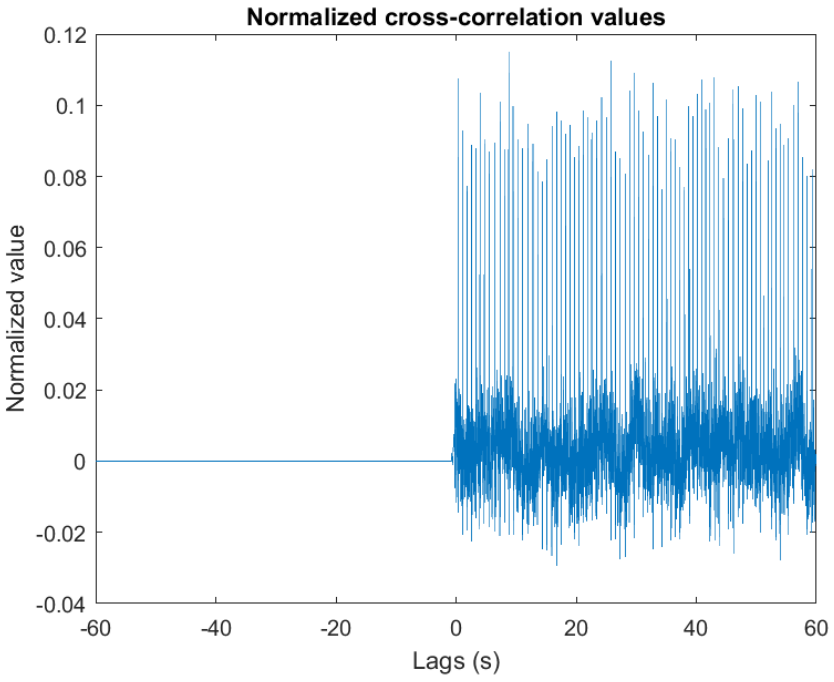

Figure 26: Normalized Cross-correlation value vs Lags

Therefore, in the following approach, the normalized cross-correlation of the 'ECG_template' signal and the 'nECG' will be calculated.

$$\Theta_{xy} = \frac{\sum_{n=1}^{N}([x(n) - \bar{x}][y(n - k) - \bar{y}])}{\sqrt{\sum_{n=1}^{N}([x(n) - \bar{x}])^2 \sum_{n=1}^{N}([y(n - k) - \bar{y}])^2}}$$

$x(n)$: nECG, $y(n)$: ECG_template, $\bar{x}$, $\bar{y}$: mean of nECG and ECG_template, k: lag, N: length of the template. In MATLAB implementation 'xcorr(x,y)' function has been used for calculating the normalized cross-correlation of the mentioned signals. Figure 26 shows the Normalized cross-correlation values concerning lags in the time domain.

Let's take the threshold value as 0.08 and the highest value of the consecutive points is collected as the highest correlation point of the segmentation procedure. Then we plot the SNR concerning the number of ECG pulses (Figure 27).

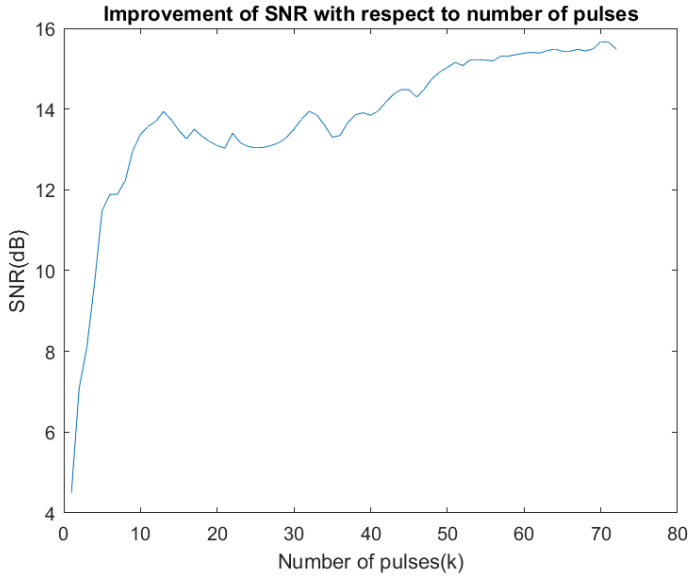

Figure 28:Improvment of SNR with respect to the number of pulses

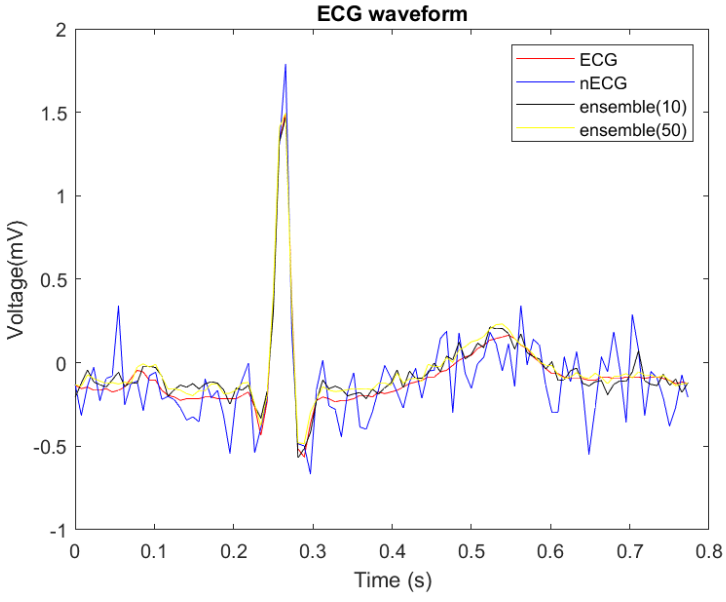

Figure 27: ECG, nECG and ensemble signals

Then we select arbitrary ensembled average pulses (10 and 50 pulses are used to calculate the ensemble average) Then compared them with ECG, nECG and ensemble(10) and ensemble(50). Ensemble(50) has more reduced noise compared to the ensemble(10). Therefore by increasing the number of pulses useful information about the signal can be obtained.

The cross-correlation method is better than the peak detection method because the length of the time may vary at different PQRST waves. Also, there are some abnormal wave rejections.

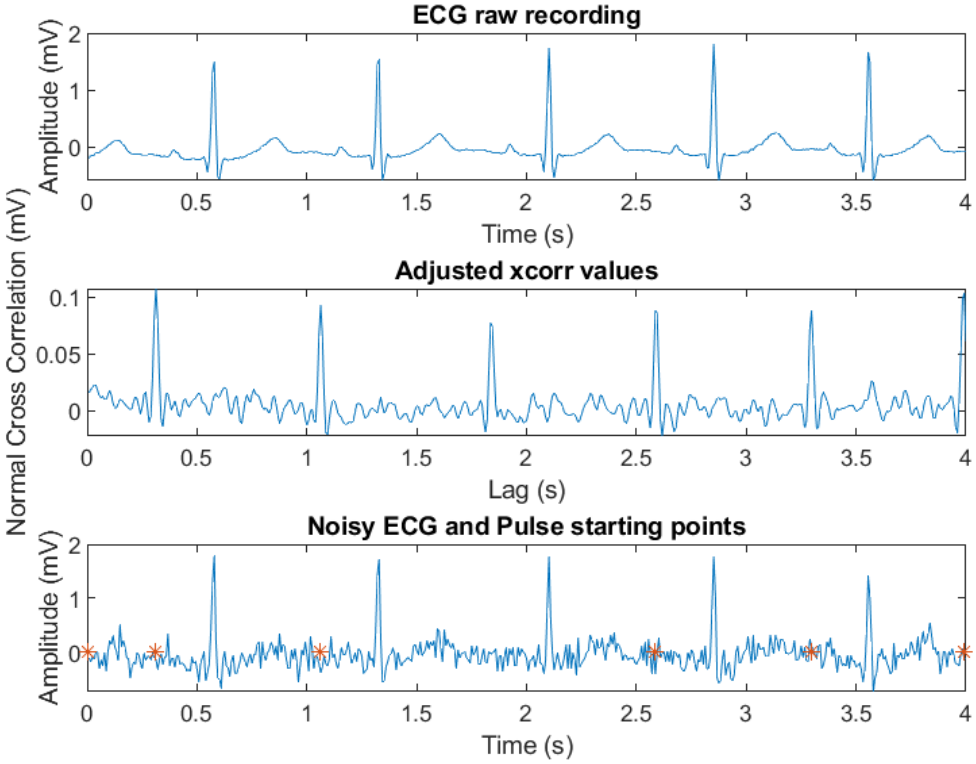

Figure 29: i) ECG raw recording ii) Adjusted xcorr values iii) Noisy ECG and Pulse starting points

Figure 29 verifies that when the template signal more coincides with the noise signal higher correlations are occurred. Therefore with the selection of a proper threshold value peak detection of cross-correlation and then pulse detection can be done accurately.

3 FIR derivative filters

3.1 3.1. FIR derivative filter properties (use the fvtool(b,a))

Different types of FIR filters can be designed by changing the filter coefficient. The filter characteristics are also changed with the filter coefficients. The following approach describes the derivative-based filters.

The first-order derivative of a discrete signal can be written as

$$y(n) = \frac{x(n) - x(n-1)}{T}$$

Here T is the sampling period. Then convert the time domain function to a frequency domain

$$Y(z) = \frac{X(z)(1 - Z^{-1})}{T}$$

Then the transfer function of the signal can be obtained as follows,

$$H(z) = \frac{Y(z)}{X(z)} = \frac{1 - Z^{-1}}{T}$$

Here there are only two non-zero coefficients are available, $\boldsymbol{b_0 = 1, b_1 = -1}$. Then consider the 3-point central difference derivative equation with a sampling period of T as follows.

$$y(n) = \frac{x(n+1) - x(n-1)}{2T}$$

Applying a time shift to the central difference then the signal can be used in a causal system.

$$y(n) = \frac{x(n) - x(n-2)}{2T}$$

The transfer function can be obtained as follows,

$$Y(z) = \frac{X(z)(1 - Z^{-2})}{2T}$$

$$H(z) = \frac{Y(z)}{X(z)} = \frac{1 - Z^{-2}}{2T}$$

The coefficients are $b_0 = 1, b_1 = 0, b_2 = -1$ and other coefficients are zero.

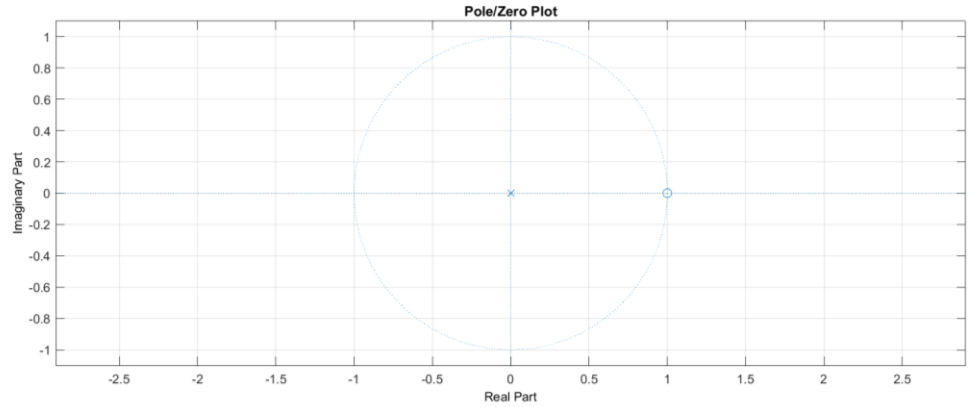

Figure 31: Pole zero Plot for 1st order filter

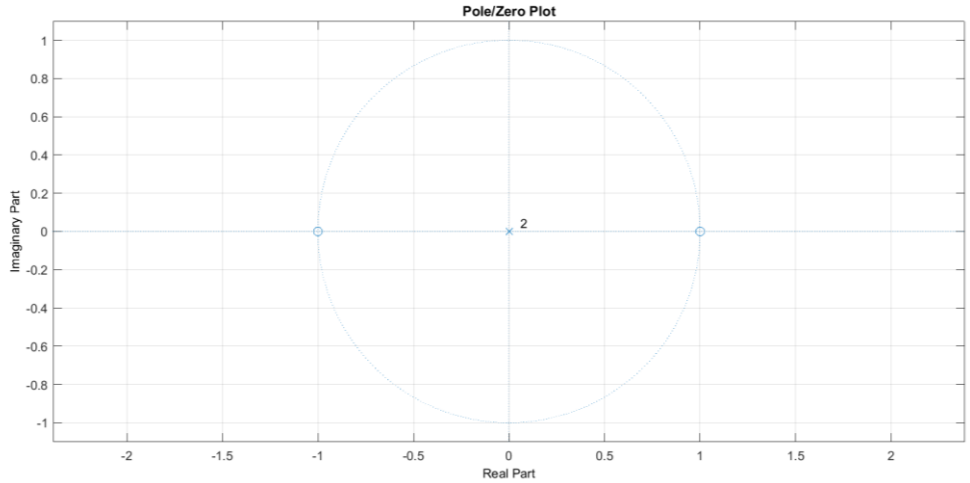

Figure 30: Pole zero plot for 3-point central difference magnitude

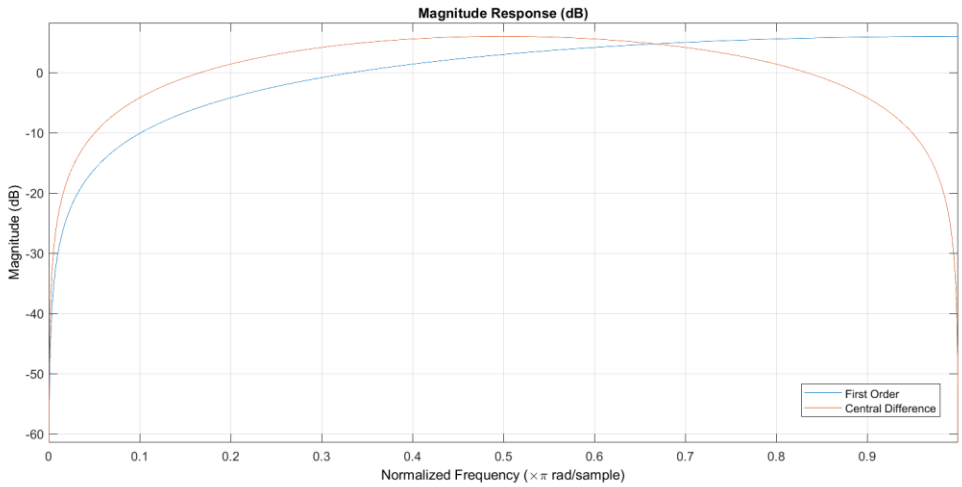

Figure 32: 1 st order and 3-point central difference magnitude response(dB)

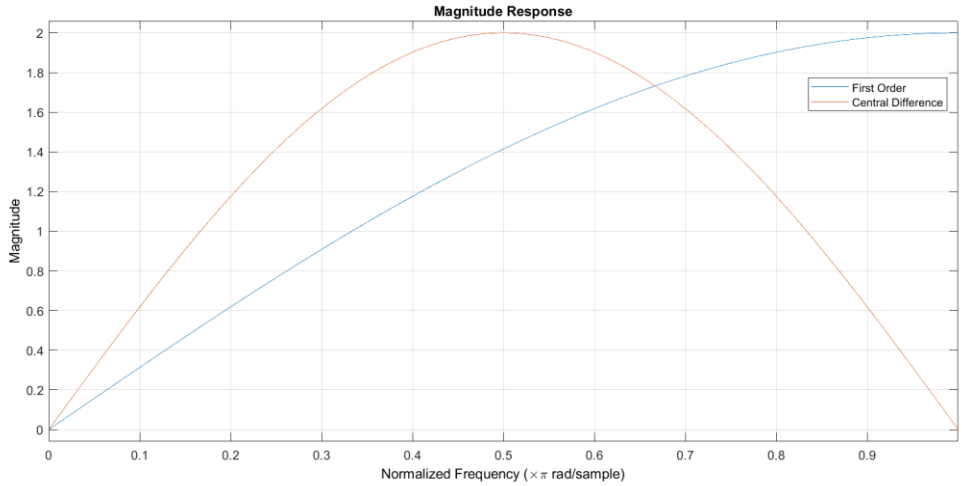

Figure 33: 1st order and 3- point central difference magnitude response

According to the above Figures, the 1 st order filter has behaved as a high pass filter and the 3-point central difference filter behaved as a bandpass filter. Also, there is an amplification of the pass-band output and it leads to making distortions in the passband. By using a scaling factor this issue can be solved and set the maximum gain to 1.

The scaling factor can be calculated as follows,

$$G = \frac{1}{\max(|H(z)|)}$$

For the first-order derivative filter,

$$|H(z)| = \frac{1}{2T}|1 - Z^{-1}|$$

When $Z = -1$, $|H(z)|$ will be maximized. Therefore

$$G = \frac{1}{\max\left(|H(z)|\right)} = \frac{T}{(|(1-(-1)^{-1})|)} = \frac{T}{2}$$

The time domain signal equation for first order derivative filter can be written as,

$$y(n) = \frac{x(n) - x(n-1)}{2}$$

For the 3-point central difference filter,

$$|H(z)| = \frac{1}{2T}|(1 - Z^{-2})|$$

When $Z = j$, $|H(z)|$ will be maximized. Therefore

$$G = \frac{1}{\max(|H(z)|)} = \frac{2T}{(|(1 - (j)^{-1})|)} = T$$

The time domain signal equation for a 3-point central difference filter can be written as,

$$y(n) = \frac{x(n) - x(n-2)}{2}$$

After adding the scaling factor no amplifications occurred. The following figures show the obtained magnitude responses after applying the scaling factor.

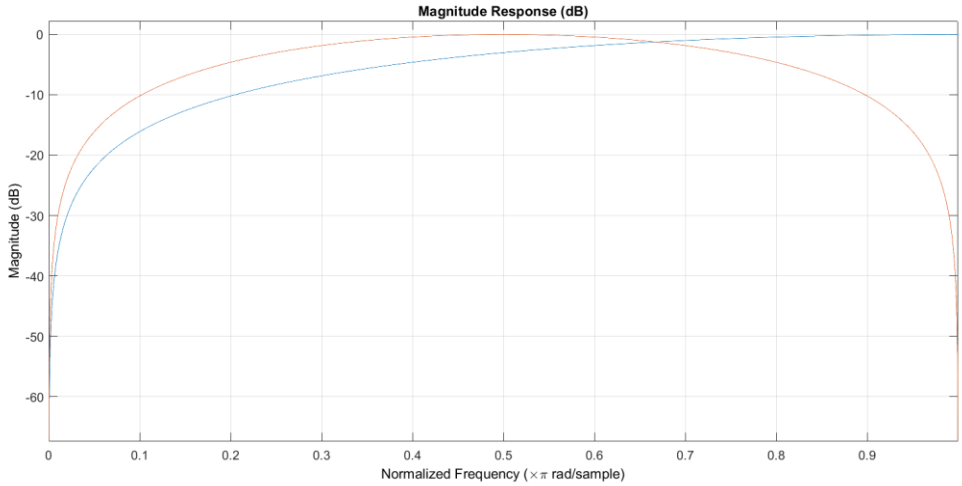

Figure 35: 1 st order and 3-point central difference magnitude response after applying scaling factors

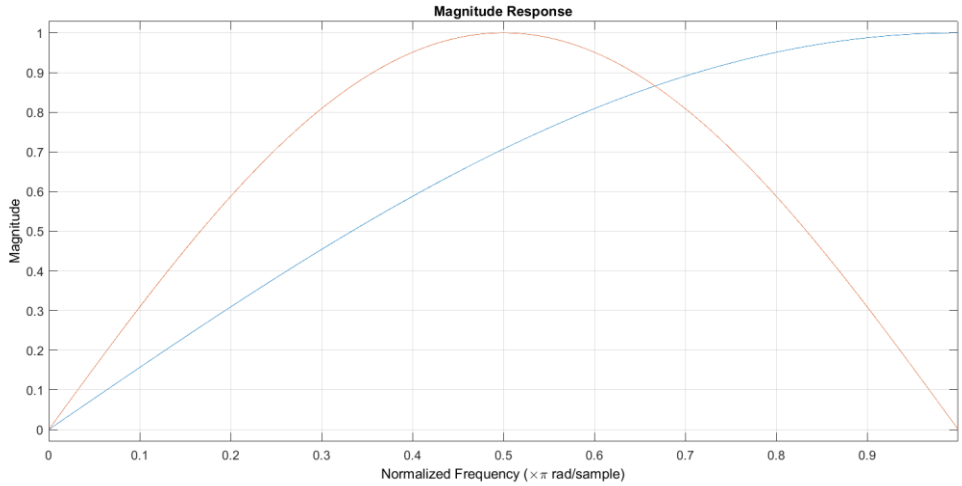

Figure 34: 1 st order and 3-point central difference magnitude response after applying scaling factors

3.2 FIR derivative filter application

In this implementation, we are adding an EMG signal and additive white gaussian noise to an ECG signal.

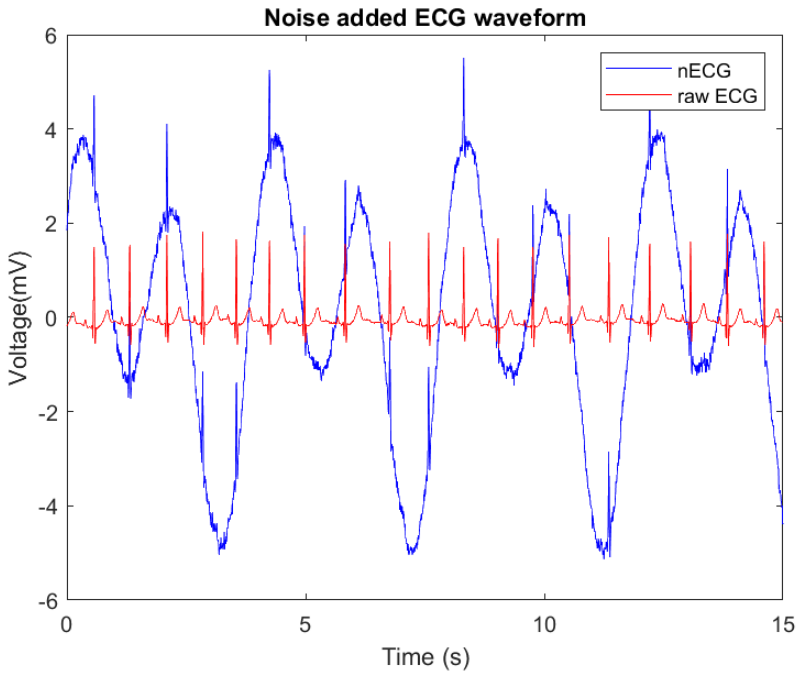

Figure 36: Raw ECG signal and noise added ECG signal

Then the previously discussed first-order filter and 3-point central difference derivative filters are applied to the noise signal. The output signals are shown in Figure 37.

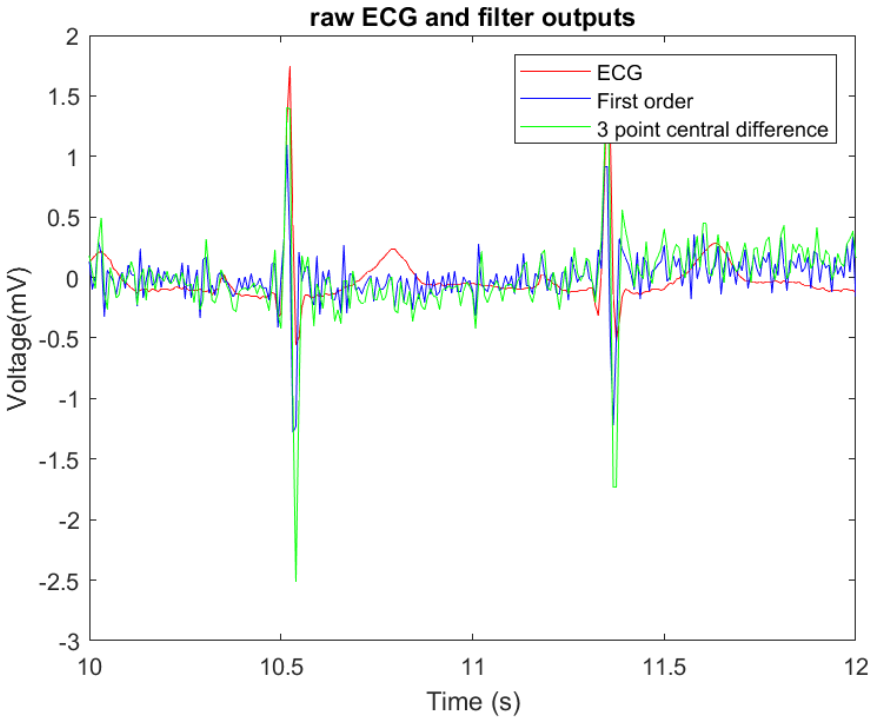

Figure 37:Output signal figures

According to the figures, both filters have filtered most of the noises but still, there are some high-frequency noise components in both filtered signals. In addition to that first-order filter has a more smoothened R complex compared to 3 points central difference filter and the first-order filter has reduced noise compared to the 3-point central difference derivative filter.

4 Designing FIR filter using windows

The window method is used to create FIR filters by windowing an ideal filter, h(n), with a window function w. (n). As a result, we can derive a finite approximation of the ideal filter. With increasing window length, an FIR filter developed in this manner approaches the perfect filter.

4.1 Characteristics of window functions (use the fdatool)

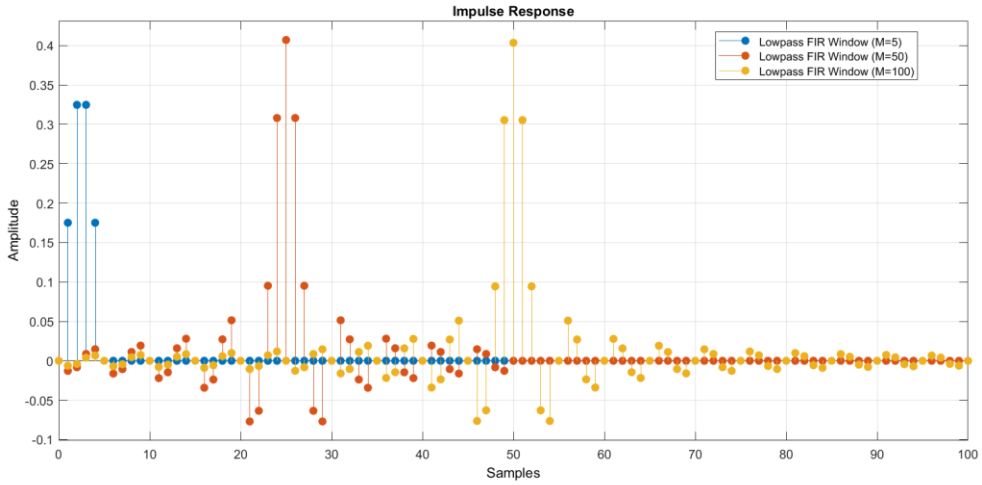

Figure 38: Impulse response for M=5,50,100 rectangular window length

Figure 38 shows the impulse response of a rectangular window when the filter order is 5, 50 and 100. When increasing the filter order filter is approximate to the ideal filter behaviour. Also, the filter smoothly filters the signal when increasing the filter order.

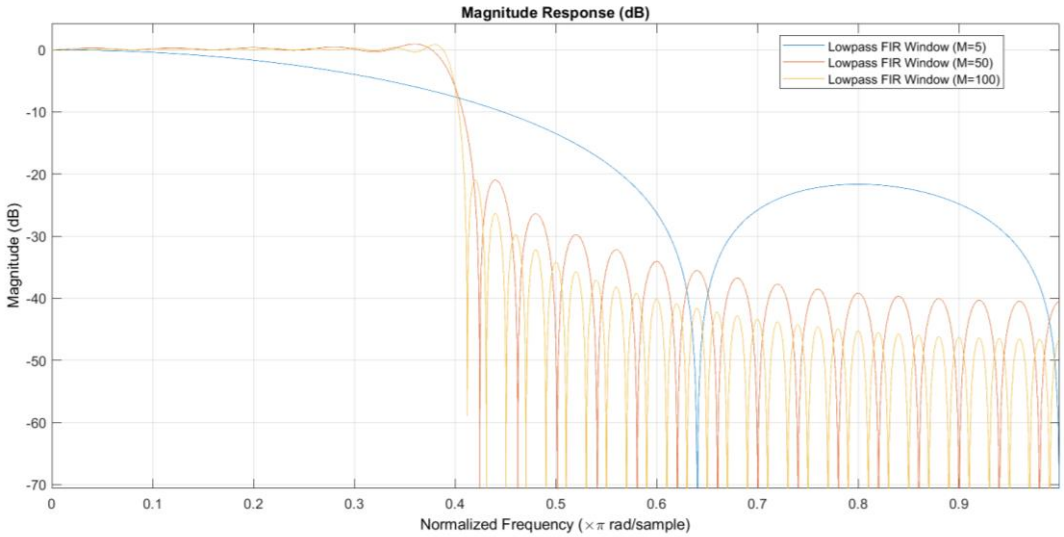

Figure 39: Magnitude response of rectangular windowing filter(dB)

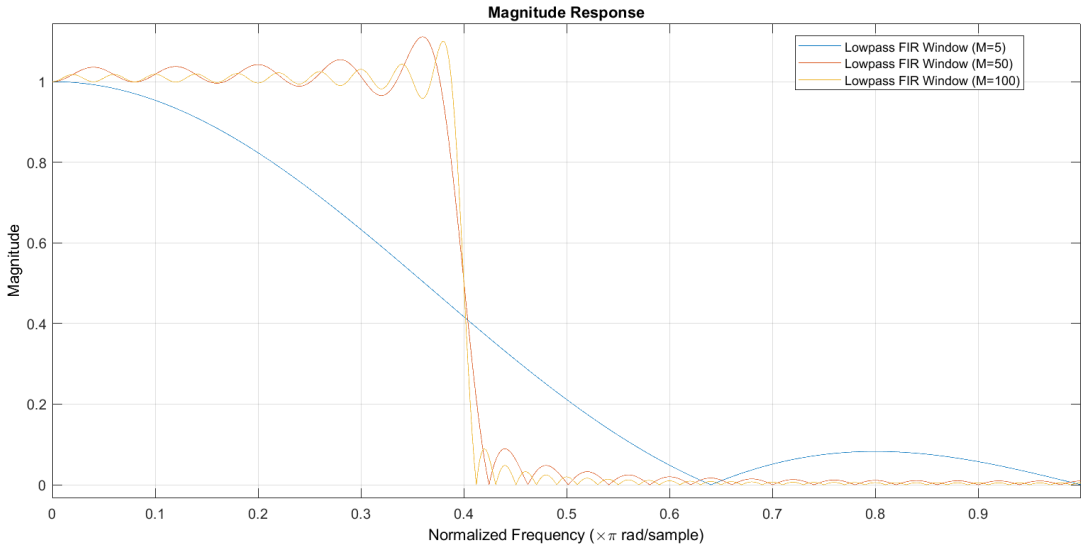

Figure 41: Magnitude response of rectangular windowing filter

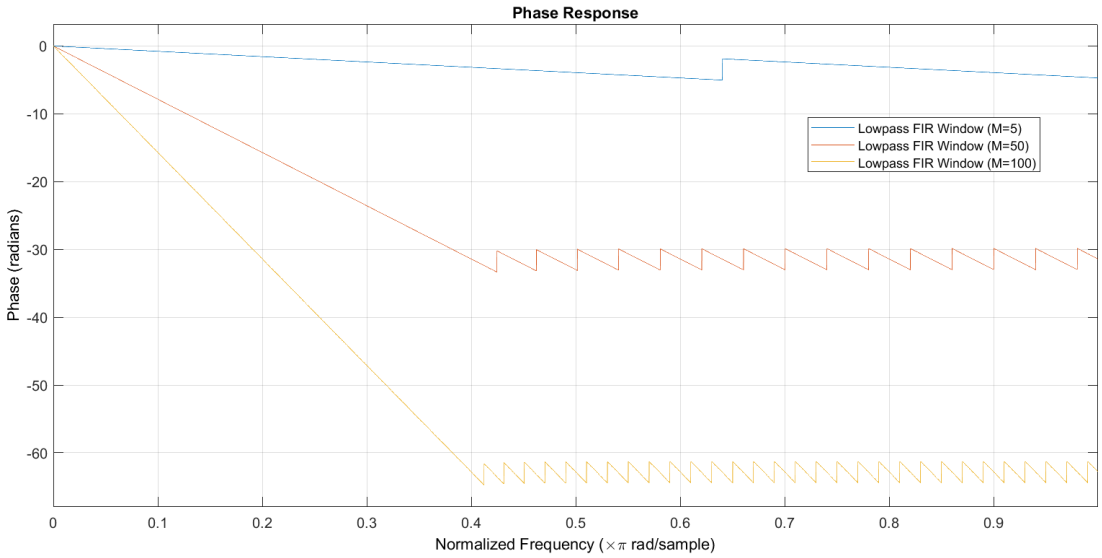

Figure 40: Phase response of Rectangular windowing filter

According to the figures when increasing the filter window length, the width of the transition period is reduced. Therefore filter has a sharper cutoff and higher attenuation when the window length is increased. The discontinuities at the edges of the rectangular window large ripple in the passband. However, increasing the filter length leads to reducing the amplitude of most ripples. The passband ripples can be removed by removing the sudden transition in the window. Different window functions have been created to make the transition smoother.

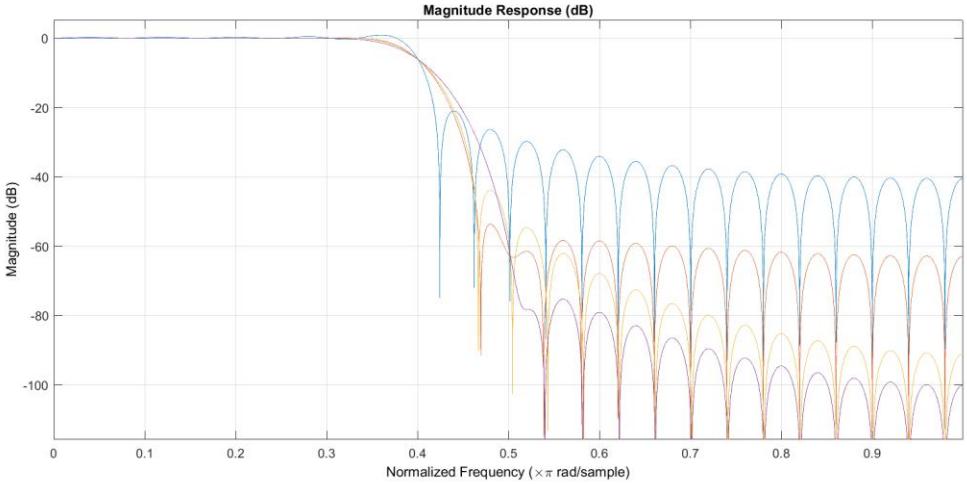

Figure 44:Magnitude Response(logarthamic scale) of diffrent filters

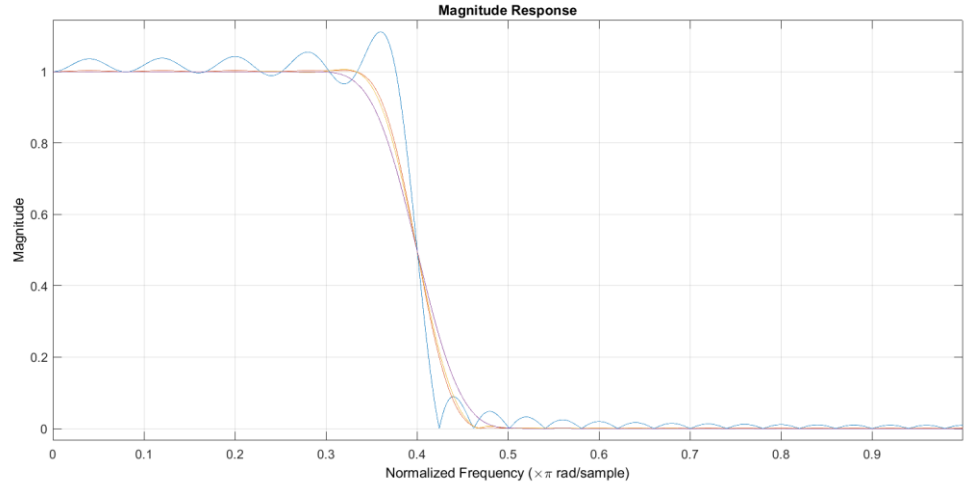

Figure 43:Magnitude Response(Linear scale) of diffrent filters

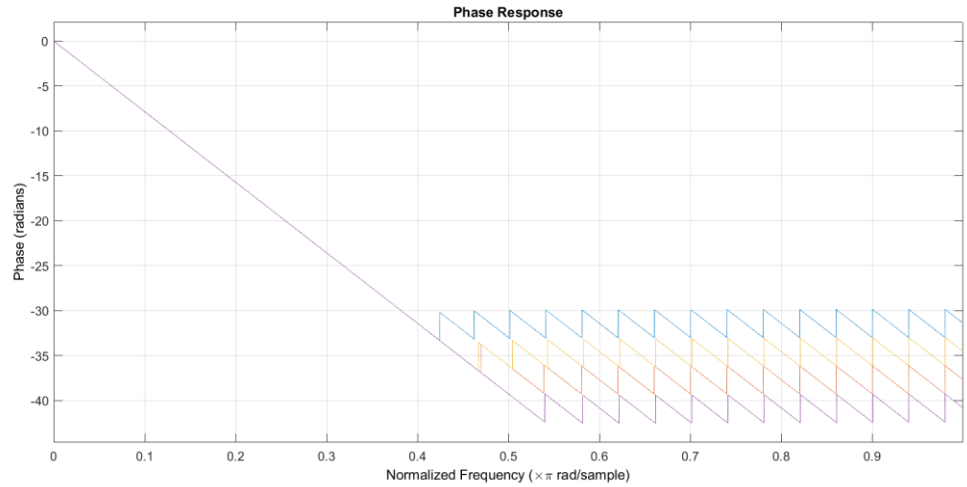

Figure 42: Phase response of the different filter

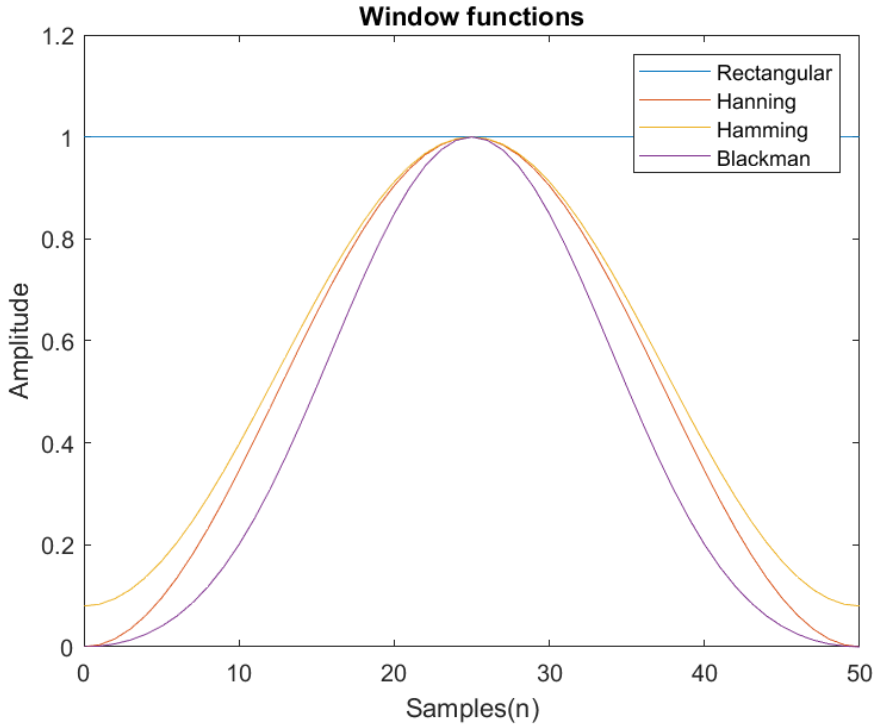

Figure 45: Moropholgies of different windows

According to the above figures the rectangular window has constant amplitudes and other window functions have bell-shaped symmetric curves. The reason for occurring ripples in the rectangular window is having constant amplitude through the window length but due to the shape of other windows, the ripples have been reduced. All filters have the same phase changes for the passband as the window length is the same.

4.2 FIR Filter design and application using the Kaiser window

For a particular window length, there is a trade-off between ripple amplitude and transition width. The Kaiser window solves the problem by adding another parameter to manipulate. This shape parameter is an arbitrary value that will be determined by passband ripple.

Consider the following noise-added signal. Figure 45 and Figure 46 represent the time domain ECG signal representation and frequency domain power spectral density.

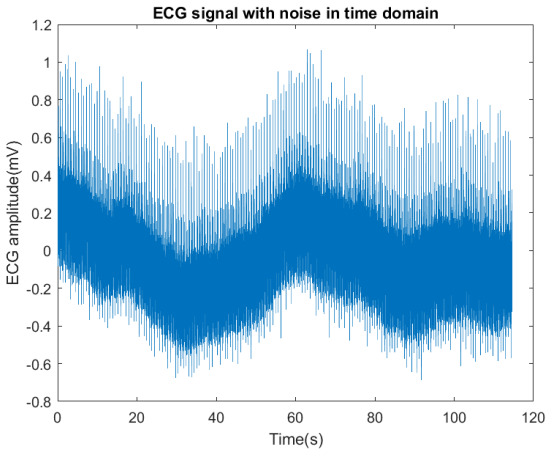

Figure 47: Noise ECG signal

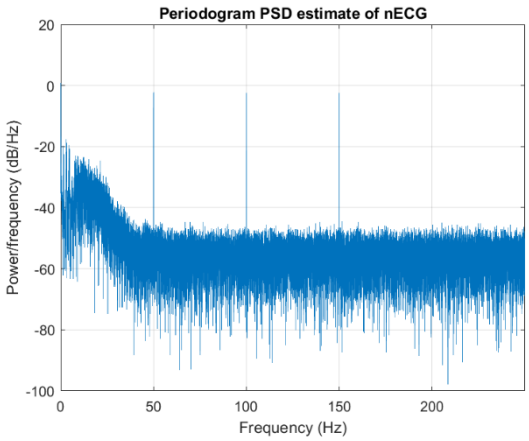

Figure 46: PSD of a noise signal

According to the above figure, the ECG signal contains high-noise components. There are three peaks at 50, 100 and 150Hz in the power spectrum. This may occur due to powerline noise.

Let ‘s create a bandpass filter and comb filter to remove the noise. The following parameters are applied to the calculation part.

	HPF(Hz)	LPF(Hz)
f_{pass}	7	123
f_c	5	125
f_{stop}	3	127
δ	0.001	

Table 1:Bandpass filter parameters

Comb filter	
f_{stop1}	50 Hz
f_{stop2}	100Hz
f_{stop3}	150Hz

Table 2: Comb filter parameters

Here we use the same transition bandwidth and max ripple amplitude for LPF and HPF filters. Kaiser window parameters are calculated as follows.

$$A = -\log\delta = -20\log(0.001) = 60dB$$

$$\Delta\omega = \left|f_{pass} - f_{stop}\right| \times \frac{2\pi}{f_s} = 0.050265$$

$$M = \frac{A-8}{2.285\Delta\omega} = 452.74$$

M is an integer, Therefore $M = 453$

$$\beta = \begin{cases} \mathbf{0.1102(A - 8.7)} & 50 < A \\ \mathbf{0.5842(A - 21)^{0.4} + 0.07886(A - 21)} & 21 \le A \le 50 \\ \mathbf{0} & A < 21 \end{cases}$$

Therefore $\beta = 5.653236$

	LPF	HPF
$\left\|f_{pass} - f_{stop}\right\|$	6Hz	
A	60	
β	5.65326	
M	454	

Table 3: Required information for filter design

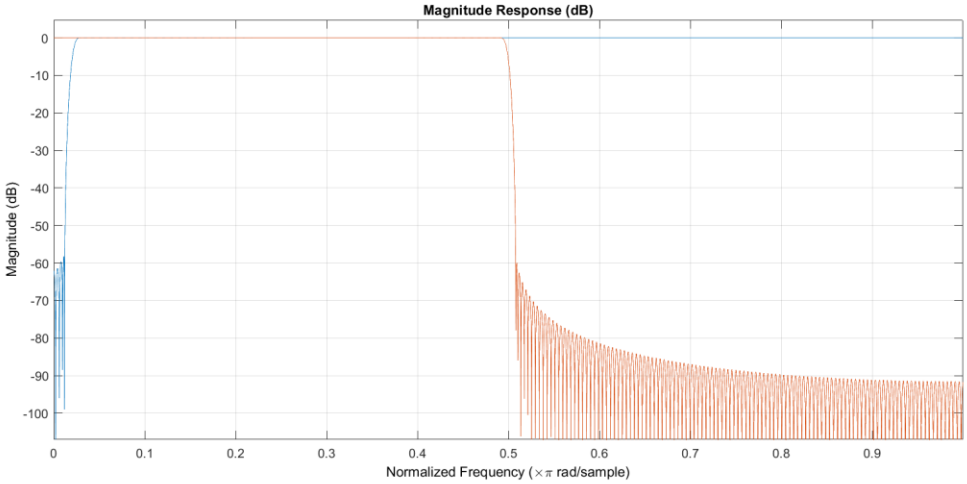

Figure 49: Magnitude response of LPF and HPF

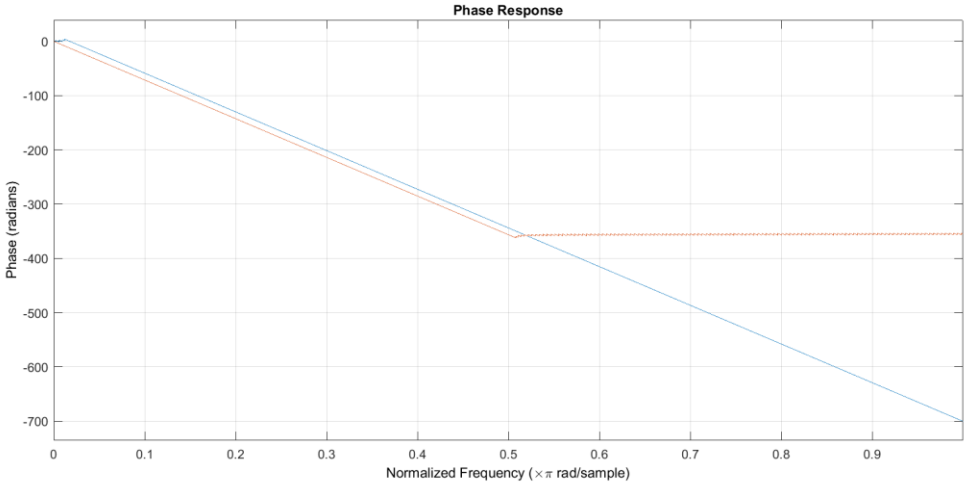

Figure 48: Phase response of LPF and HPF

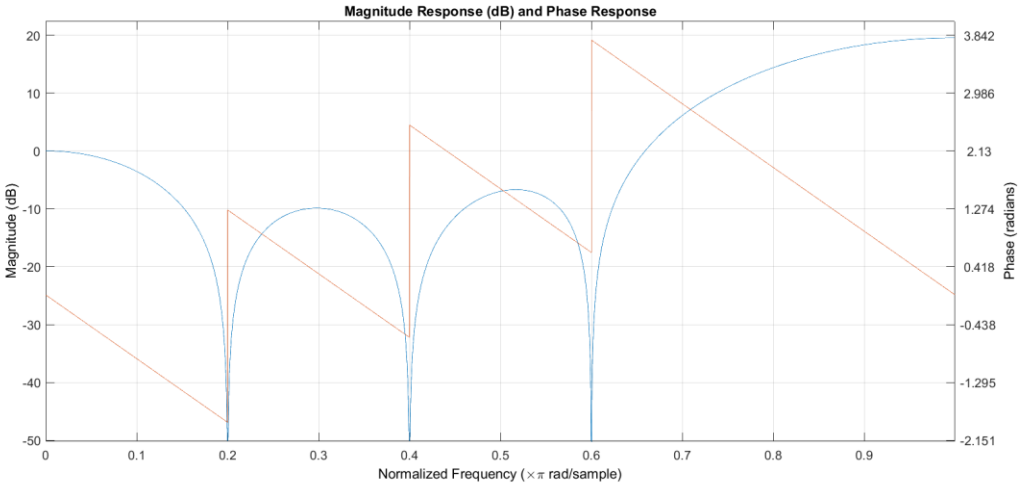

Figure 50: Magnitude Response and phase response of comb filter

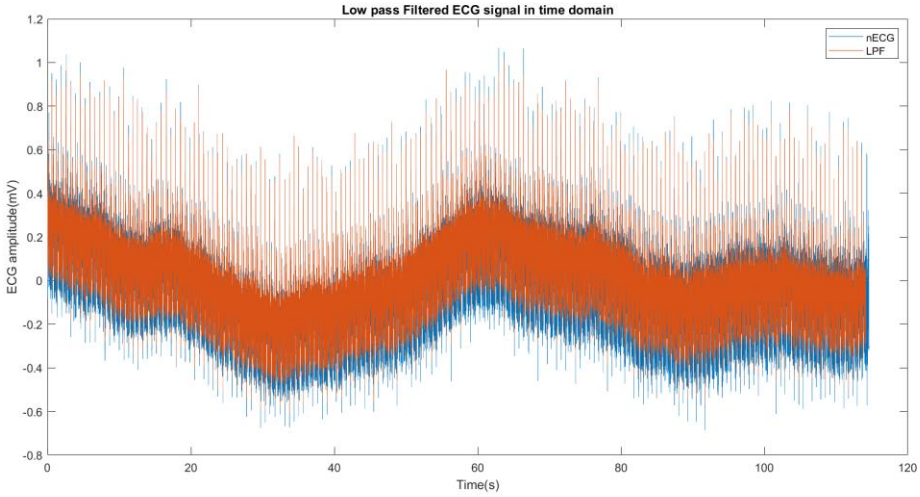

Figure 51: LPF response for the signal

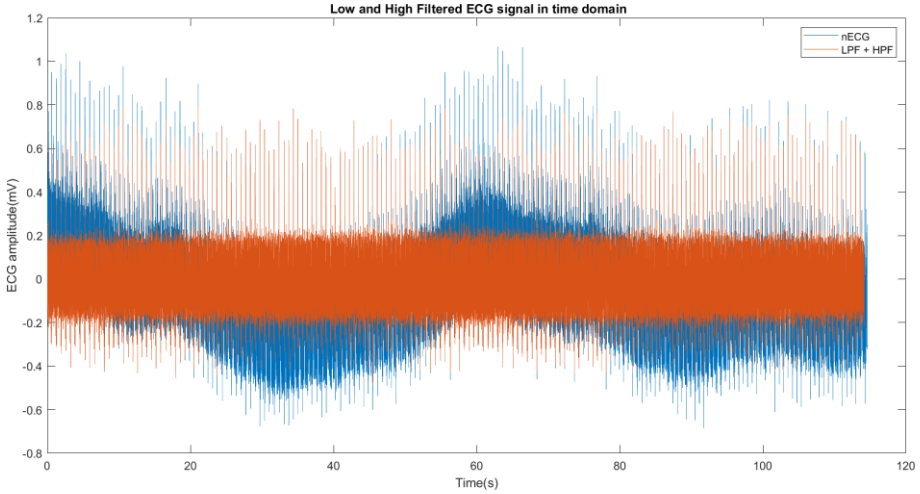

Figure 53: LPF +HPF respose for the signal

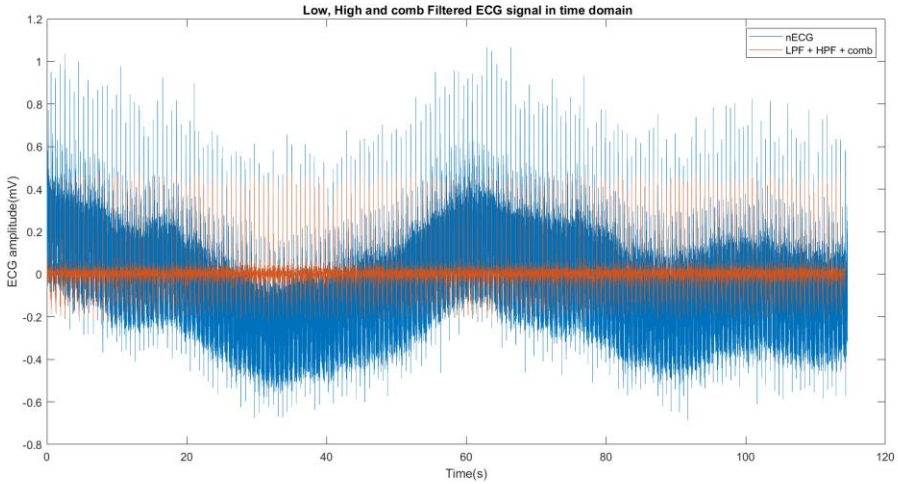

Figure 52: LPF + HPF +Comb filter response for the signal

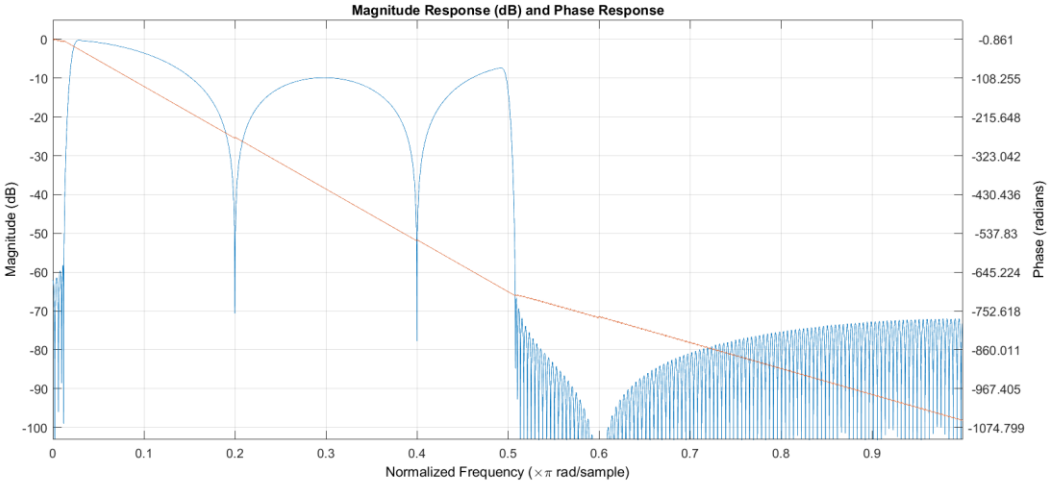

Figure 55: Magnitude and Phase response of the combined filter

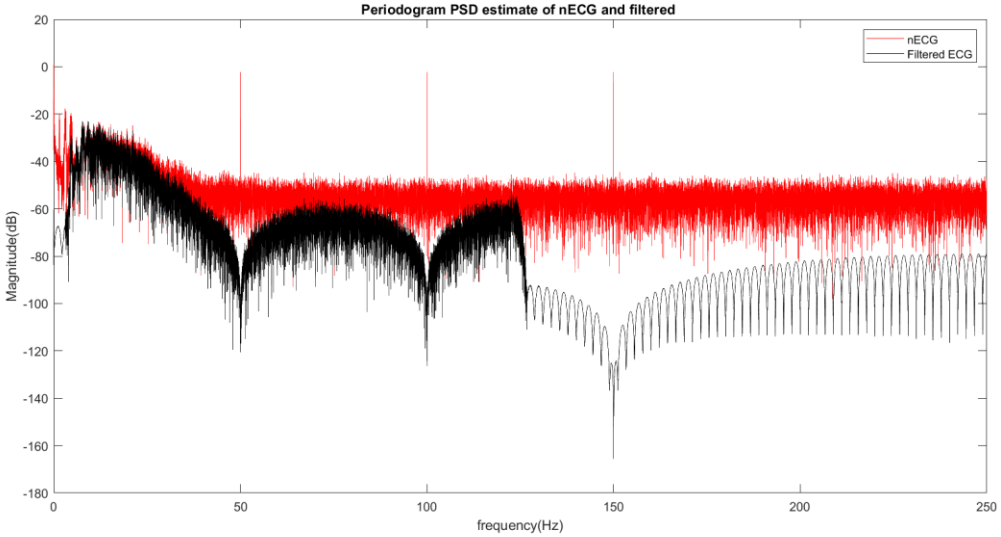

Figure 54: PSD of nECG signal and filtered ECG signal

5 IIR filters

5.1 Realising IIR filters

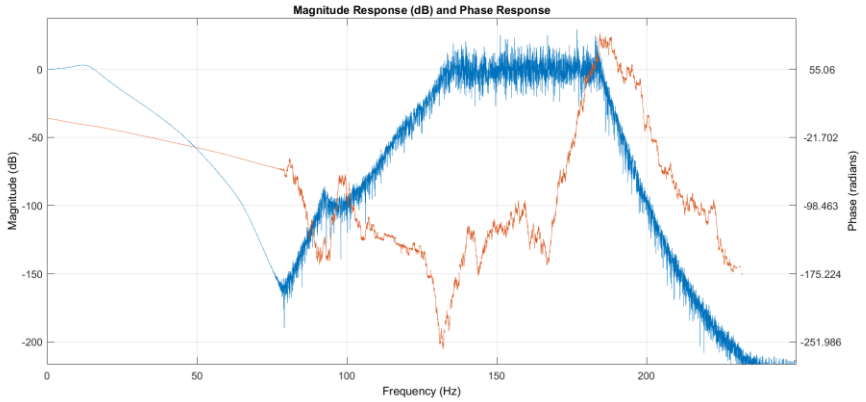

Figure 56: Butterworth filter (order=454)Response

According to the above Figure56 obtained Butterworth filter order(N) = 454 is unstable and has many frequency distortions. When higher-order IIR filters are directly implemented, there may be issues with stability and frequency distortion. This is due to problems in coefficient quantization, rounding off, and overflow when working with a finite amount of bits. This is why the frequency response of the higher-order Butterworth filter is not as predicted. Therefore let's consider M=10 for continuing the next further parts.

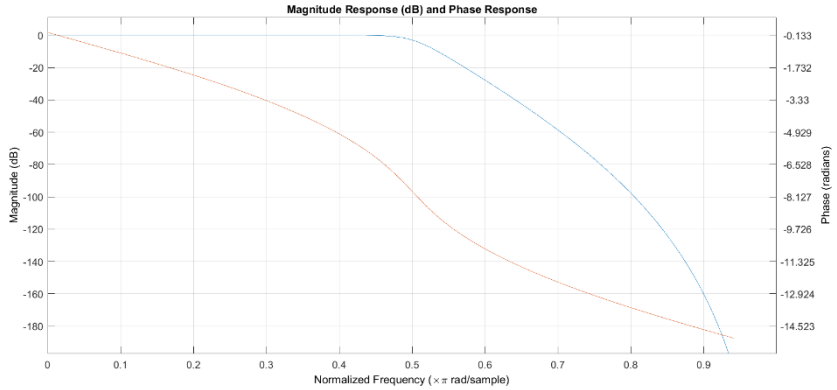

Figure 59: Butterworth filter(N=10) LP filter response

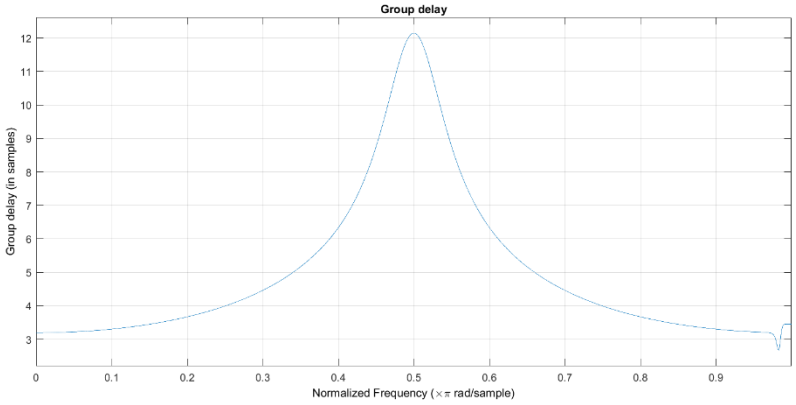

Figure 58: Group delay of the Butterworth filter(N=10)

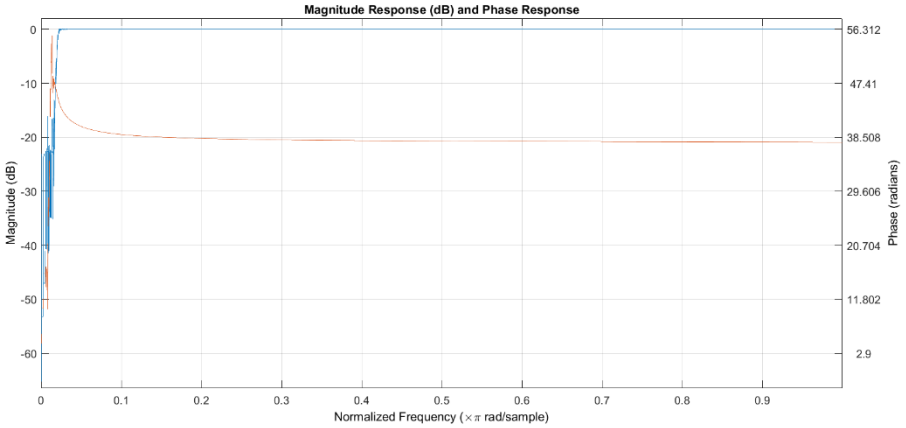

Figure 57: Butterworth filter (N=10) HPF responses

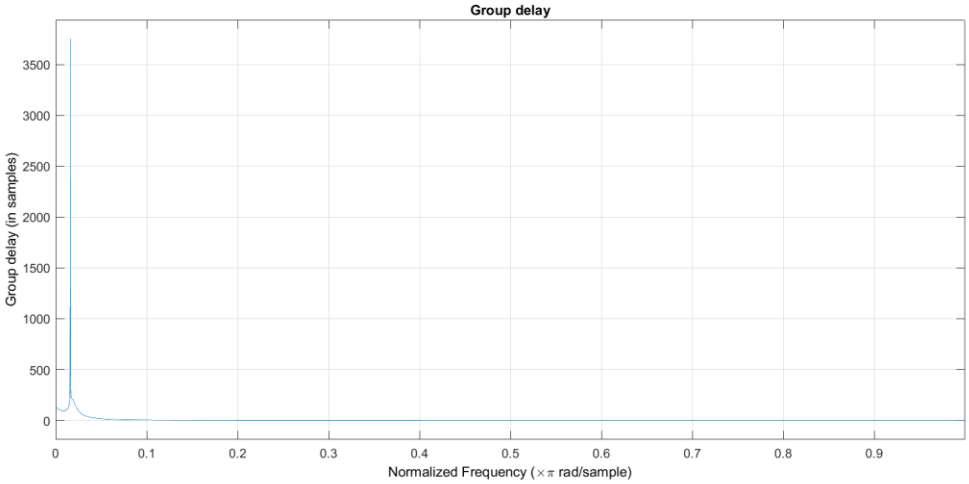

Figure 62: Butterworth filter(N=10) HP filter group delay

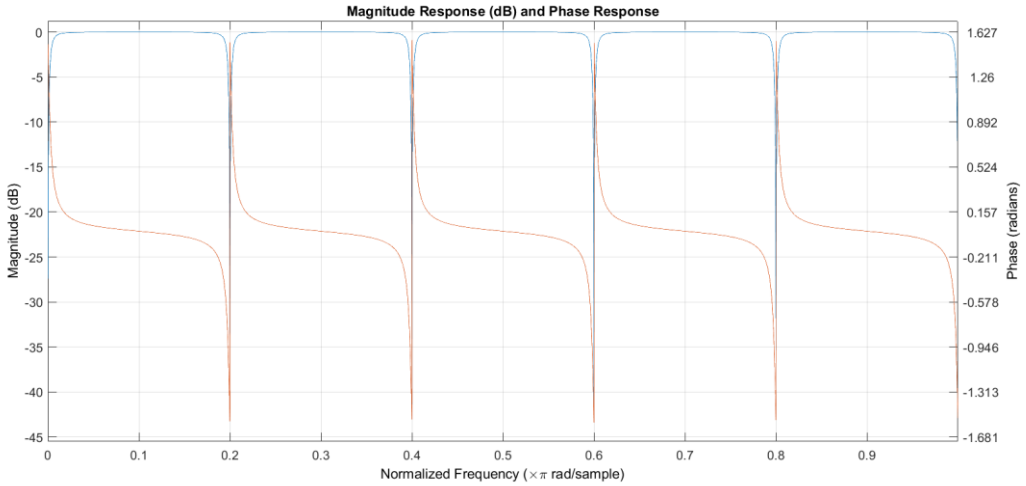

Figure 61: IIR comb filter(N=10) responses

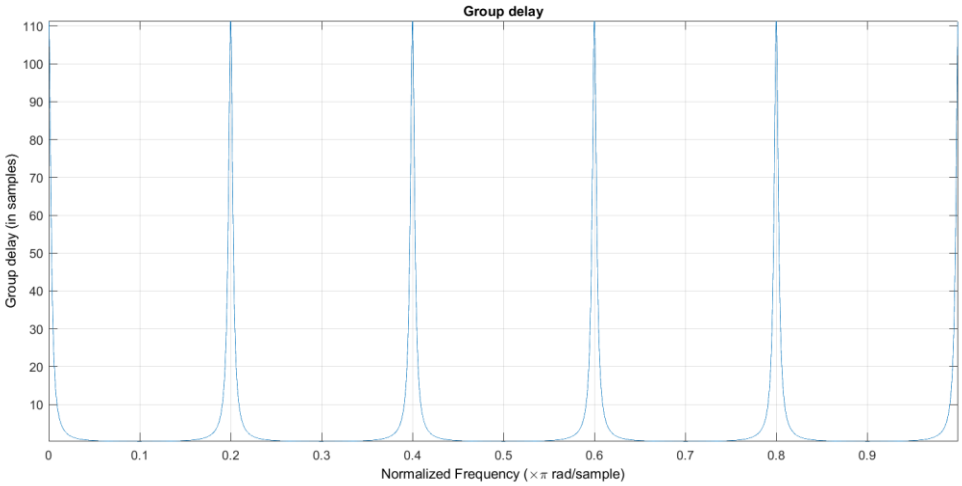

Figure 60:IIR comb filter(N=10) group delay

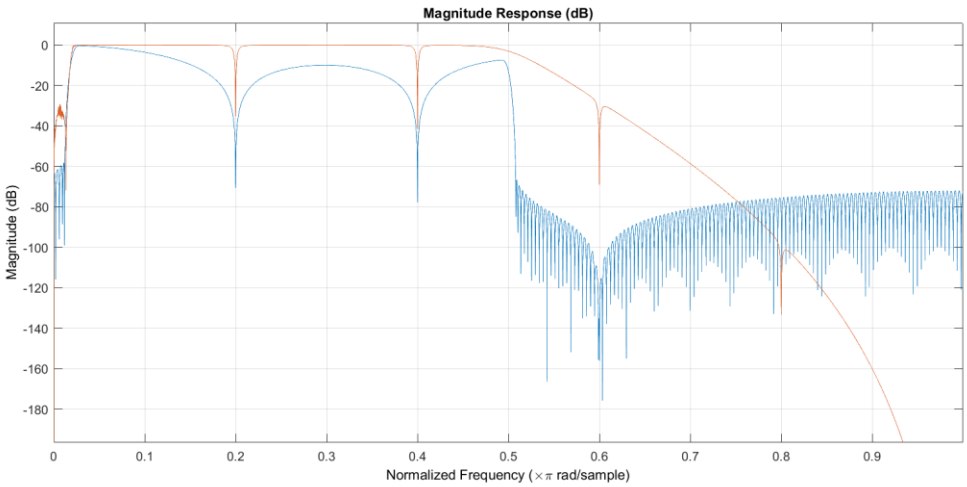

Figure 63:FIR and IIR filter magnitude and phase responses

IIR filters are a class of filters having a recursive feedback mechanism that display non-linear phase inside the passband. While often having an unlimited impulse response, this combination of filters is not always stable. IIR filters typically have better comparable to FIR filters of the same order in terms of frequency response. When directly implementing higher-order IIR filters, stability and frequency distortion problems frequently occur that prevent the frequency response from being what is needed. These problems are caused by errors in coefficient optimization, rounding off approximations, and overflow errors because of calculations involving a finite number of bits. By cascading several second-order sections or other smaller-order filters, these problems could be resolved. Since MATLAB's direct implementation of Butterworth seems unstable at orders above 10, a lower-order filter, such as the 10th order Butterworth filter

5.2 Filtering methods using IIR filters

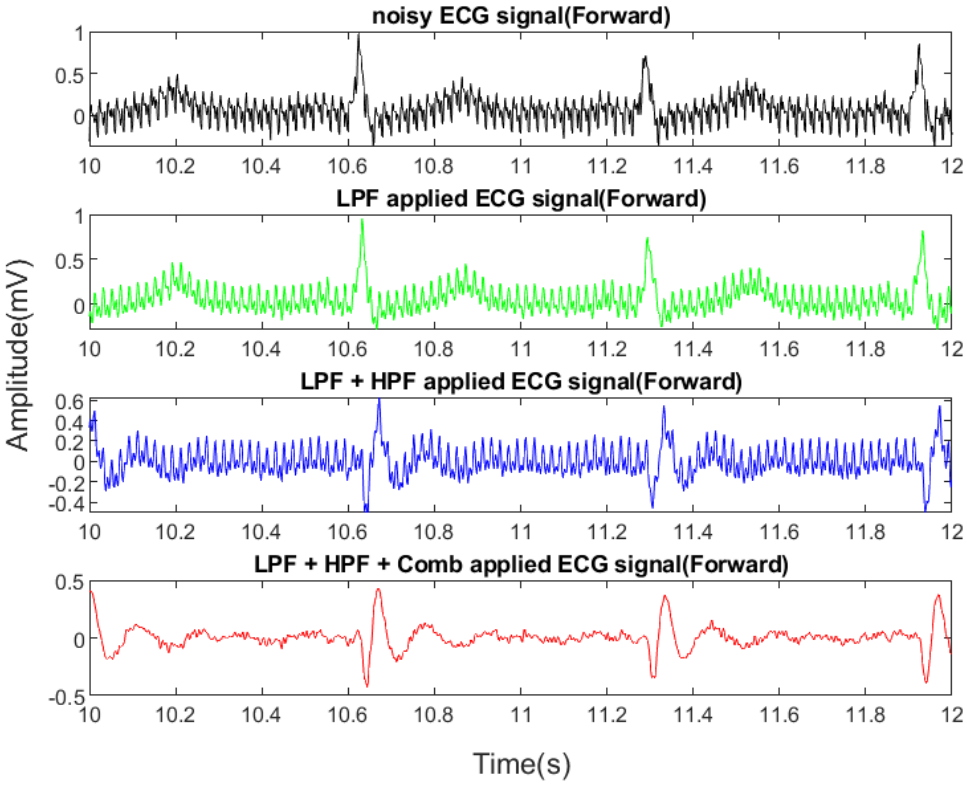

Figure 64: forward filtered ECG

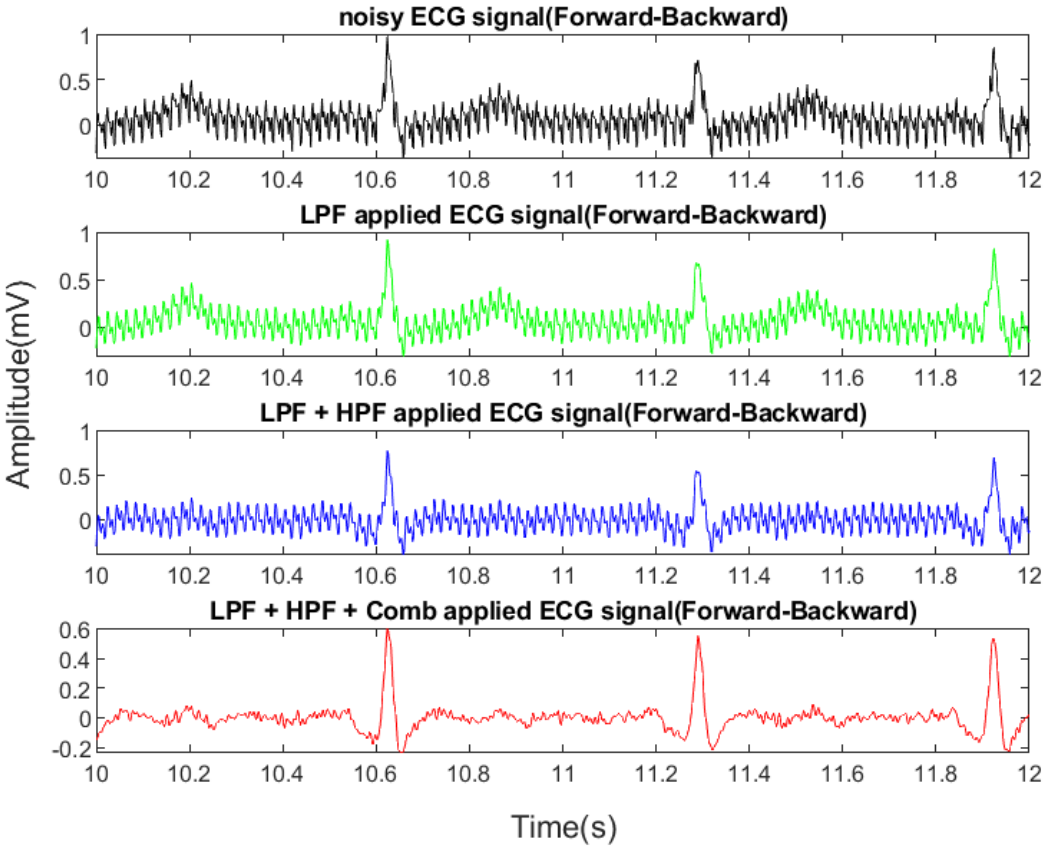

Figure 66: Forward-backward filterd ECG

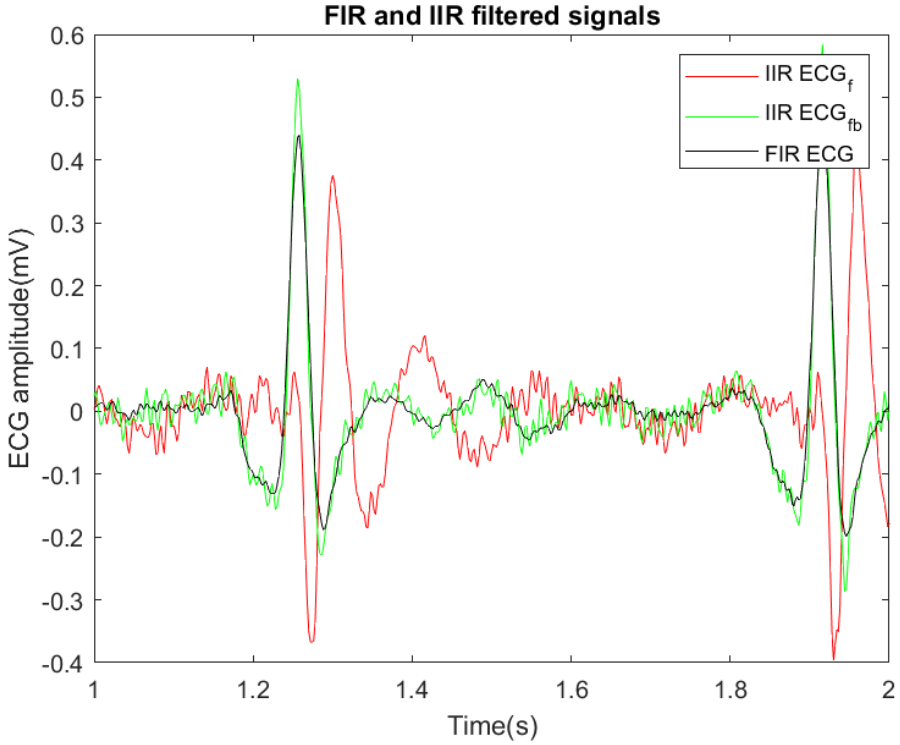

Figure 65:FIR and IIR filter outputs

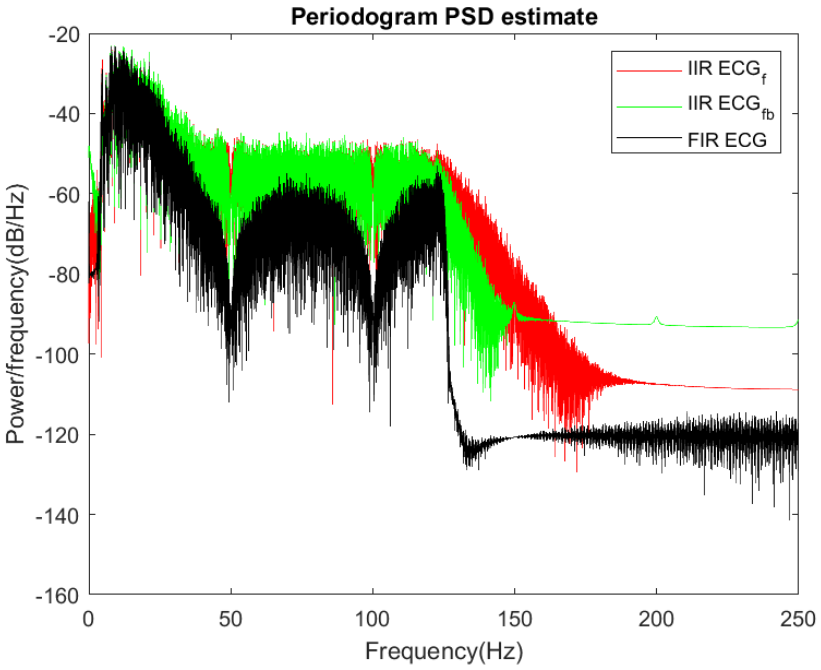

Figure 67:PSD's of FIR and IIR filtered signal

As can be seen, the IIR filter has a higher amplitude response in the pass band than the FIR filter. Furthermore, the notch filter features have a narrower bandwidth than the FIR despite having strong stopband attenuation (in IIR). The transition bandwidth in the IIR filter, on the other hand, is larger (due to the lower order) than in the FIR filter. Furthermore, despite its superior frequency response, the IIR filter exhibits a non-linear response in the passband. However, if the complete needed signal is saved, forward-backwards filtering via a secondary backward filtering procedure could be used to achieve zero phase response, as seen in the time and frequency domain charts.